Trimethylenemethane Derivatives Stabilized by Conjugation II − Concerted or Nonconcerted Generation?[‡]

Wolfgang R. Roth,*[a][†] Holger Wildt,[a] and Andreas Schlemenat[a]

Keywords: Heats of formation / Pericyclic reactions / Radicals / Reaction mechanisms / Thermodynamics

The concerted formation of the orthogonal trimethylene-type diradicals **3**, **6**, and **12** has been demonstrated for the three homofulvenes **2**, **4**, and **7** and shown to proceed preferentially in a disrotatory manner. The same type of orthogonal diradicals are formed, but in a nonconcerted fashion, from the bicyclic methylenecyclopropanes **26**, **30**, **33**, and **40**, through the planar diradicals **28**, **31**, **35**, and **50**, respectively. The different reaction modes are viewed as being caused by the different coupling probabilities of the underlying vibrations. The orthogonal or planar geometries of the diradicals were derived from stereochemical and kinetic arguments. Additional thermodynamic characterization was achieved for three diradicals [**3c**, (*E*)-**19**, and **41**] by oxygen-trapping experiments.

All reactions dealing with the formation or cleavage of more than one bond present the question of the chronology of these events. Do they occur simultaneously or step by step? In the first case the reaction is concerted, in the second it is a multi-step process. By definition, the differentiation is thus purely phenomenological.

The vast majority of concerted reactions are found in the pericyclic reactions, and the two terms "concerted" and "orbital symmetry allowed" are therefore frequently used synonymously, as these latter reactions have to be concerted in nature, in contrast to those reactions that are not directed by orbital symmetry. However, this usage is unfortunate, because nonpericyclic reactions can be concerted as well. Examples are the fragmentation reactions studied intensively by Grob[2] and the decomposition of azo compounds.[3]

Because of this equating of "concerted" with "allowed" processes, the former reaction channel became considered to be thermodynamically favored. However, this assumption is questionable. We have to take into account that, among nonpericyclic reactions, the concerted pathway is the exception and not the rule. This prompts the question of which factors are responsible for the concerted or nonconcerted course of a reaction.

This work examines that question for a particular case, namely the generation of the trimethylenemethane diradical starting from different precursors. In agreement with theory, the orthogonal geometry **1b** is favored over the planar structure **1a** in the singlet state by 2−6 kcal·mol^{-1}. The same order is also observed for trimethylenemethane derivatives.[1] Nevertheless, both occurrences − the direct formation of the orthogonal diradical and the formation of the planar diradical, which then rearranges to the thermodynamically favored orthogonal isomer in a second step − may be observed, depending on the precursor. The latter isomerization sometimes requires a substantial activation energy.[1] A comparison of the geometry of the substrate and that of the initially generated trimethylenemethane should provide information about the decisive factors that determine the one- or two-step nature of the reaction pathway.

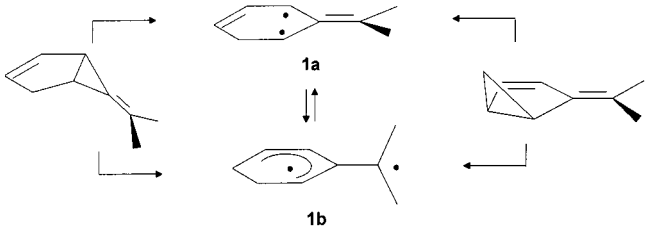

1. Homofulvene (2)

On the basis of kinetic arguments we had postulated that ring opening in the course of the geometric isomerization of the homofulvene (*E*)-**2** ⇄ (*Z*)-**2** immediately affords the orthogonal diradical **3**.[1] Compelling evidence supporting this assumption should be obtainable from thermolysis of optically active derivatives. Whereas any reaction mechanism passing through the planar diradical would cause racemization, preservation of the optical activity would demonstrate that the (*E*)-**2** ⇄ (*Z*)-**2** rearrangement was proceeding by way of the orthogonal diradicals (*R*)-**3** or (*S*)-**3** (Scheme 1).

Separation of the enantiomers was performed by HPLC. The enantiomers of (*E*)-**2a** and (*Z*)-**2a** were obtained in *ee*s of 92% and 85%, respectively, using a triacetylcellulose column. Thermolysis of pentane solutions of either the (*E*) or the (*Z*) isomer at 170 °C gave rise to the formation of the

[‡] Preceding part: See ref.[1]
[†] Deceased October 29, 1997; any correspondence should be addressed to H. Wildt.
[a] Fakultät für Chemie der Universität Bochum
Postfach 102148, 44780 Bochum, Germany
Supporting information for this article is available on the WWW under http://www.wiley-vch.de/home/eurjoc or from the author.

  1434−193X/01/1121−4081 $ 17.50+.50/0

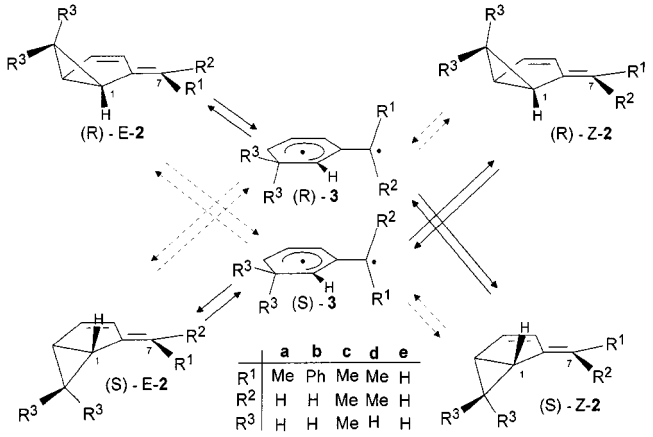

Scheme 1. Mechanism of racemization and geometric isomerization of **2**

other three isomers. All four compounds could be separated by GC on a perpentylated cyclodextrin column. The product distribution, extrapolated to $t = 0$, is shown in Table 1.

As shown in Table 1, the geometric isomerization of the homofulvene proceeds with preservation of the optical activity of the substrate in the products. The racemization of the substrate is the slowest reaction. Therefore the geometric isomerization cannot have passed through the planar, achiral diradical. However, as the isomerization takes place by way of the orthogonal diradicals (*R*)- and (*S*)-**3**, the product distribution can be explained effortlessly: The steric interaction between the hydrogen atom at C-1 and the substituent at C-7 that is directed towards the three-membered ring is the decisive force. Depending on the approach of the hydrogen atom, coming from below or above the plane of the five-membered ring, the substituent at C-7 moves up or down to yield (*R*)- or (*S*)-**3**. Recombination of the radicals takes place in the same manner. The substituent moving into the plane pushes the hydrogen atom at C-1 up or down, causing the selective formation of the enantiomeric rearrangement products. The main product is therefore the geometric isomer possessing an inverted three-membered ring and the product present in smallest concentration should be the enantiomer of the substrate.

Similarly, an analogous product distribution is observed in the thermolysis of optically active **2b**[1] (Table 1). The preference for the formation of the geometric isomer with an inverted three-membered ring can be calculated from the temperature-dependence of the product distribution, determined between 140−180 °C and extrapolated to $t = 0$. It is found to be $\Delta\Delta H^{\ddagger} = 0.8$ kcal·mol^{-1} relative to the product with retained stereochemistry and $\Delta\Delta H^{\ddagger} = 1.3$ kcal·mol^{-1} relative to the racemization product. This interpretation of the selectivity is similar to the gear mechanism studied by Mislow,[4] which is discussed later.

2. Benzohomofulvene (4)

With the aim of confirming the selective opening of the homofulvene **2**, we have also analyzed the stereochemistry of the ring opening of the benzo derivative **4**. Its synthesis was achieved by Wittig reaction, starting from the corresponding ketone **5**.[5] The (*E*) isomer could be separated into its enantiomers by HPLC through a triacetylcellulose column, yielding (−)-**4** with an *ee* of 98%.

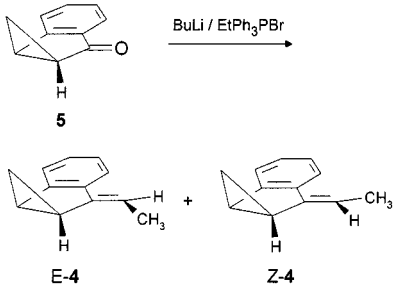

At 160 °C, thermolysis of the optically active (*E*) isomer gave rise to racemization and geometric isomerization (Scheme 2). All four isomers can be separated by gas chromatography, using a perpentylated cyclodextrin column. The product distribution, extrapolated to $t = 0$, is shown in Table 1.

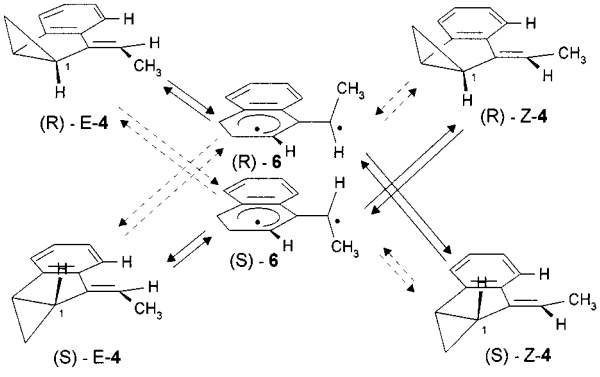

Scheme 2. Mechanism of racemization and geometric isomerization of **4**

Table 1. Primary product distribution in the thermolysis of **2a**, **2b**, and **4**

Substrate	(+)-(*E*)-**2** [%]	(−)-(*E*)-**2** [%]	(+)-(*Z*)-**2** [%]	(−)-(*Z*)-**2** [%]
(+)-(*E*)-**2a**	−	2	6	92
(+)-(*E*)-**2b**[4]	−	15	23	62
	(+)-(*E*)-**4** [%]	(−)-(*E*)-**4** [%]	(+)−(*Z*)-**4** [%]	(−)-(*Z*)-**4** [%]
(−)-(*E*)-**4**	21	−	71	8

The observed product distribution can once again be explained by considering the steric interaction between the exocyclic double bond substituent and the hydrogen atom at C-1 of the three-membered ring. The main product should again be formed by inversion both of the cyclopropane ring and of the configuration of the double bond. Nevertheless, the enantiomer of the substrate is no longer the product with the smallest concentration, most probably because of the unfavorable interaction with the hydrogen in the *peri* position of the aromatic ring in (*Z*)-**4**.

3. 2-Alkenylidenebicyclo[3.1.0]hex-3-ene (7)

If the formation of the orthogonal diradicals **3a** and **6** in the thermolysis of the homofulvenes **2a** and **4** is indeed steric in nature, then its generation should be forestalled in the alkenylidene system **7**, in which any directing interaction between the cyclopropane hydrogen and the substituent on the double bond is precluded.

The synthesis of the alkenylidene compound was achieved as outlined in Scheme 3. Addition of propylidenecarbene to cyclopenten-3-ol resulted in **9**, which was transformed into the corresponding selenide. Oxidative elimination at 0 °C yielded **11**, which rearranged at room temperature into a mixture of the alkenylidene compounds (*E*)-**7** and (*Z*)-**7**. Separation of the enantiomers was achieved by HPLC with a triacetylcellulose column, yielding the enantiomers in optically pure form. The (*E*)/(*Z*) stereochemistry of **7** could not be assigned unequivocally by spectroscopic methods.

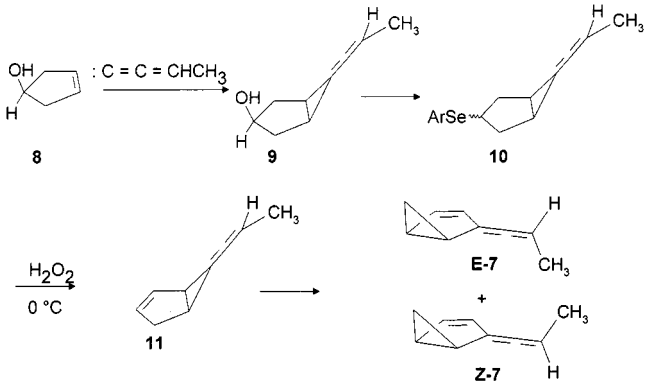

Scheme 3. Synthesis of 2-propenylidenebicyclo[3.1.0]hex-3-ene (**7**)

The thermolysis of the pure enantiomers was carried out in pentane solution at six different temperatures (170−220 °C). Three products were formed in each case: the geometric isomer and the two enantiomers of the (*Z*) and the (*E*) compound. GC analysis using a perpentylated cyclodextrin column allowed all four compounds to be observed separately, imbuing the kinetic measurements with a high degree of reliability.

The reactions shown in Scheme 4 can be described phenomenologically by three first-order rate constants (Table 4). These were determined by simulation of the reactions outlined in Scheme 4 and fitting of the rate constants to the experimental concentration/time curves using a Simplex routine.[5]

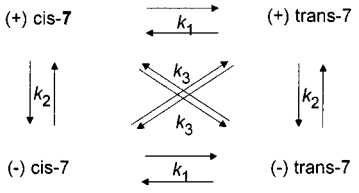

Scheme 4. Rate constant for the isomerization of **7**

The similarity of the activation parameters resulting from k_2 and k_3, contrasted with the distinctly different ones from k_1, is striking. This could indicate that the two former rates describe the process associated with a change of the configuration of the allenic unit, whereas the latter is responsible for the inversion of the three-membered ring.

Convincing evidence supporting this assumption comes from the observation that (*S*)- and (*R*)-**7** are formed in unequal concentrations. Thus the "orthogonal" diradicals **12** cannot be the only intermediates in the isomerization (Scheme 5). Were this the case, the enantiomers of the rearrangement product would have to be formed in equal concentrations. A competing reaction pathway by way of the "planar" diradical **13** is hence required. The major geometric isomer must include molecules produced by the inversion of the cyclopropane ring.

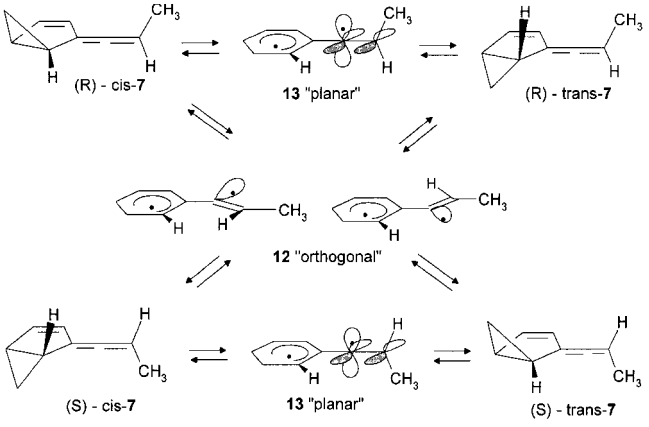

Scheme 5. Mechanism of racemization and geometric isomerization of **7**

The most important result of the thermolysis is the preference for geometric isomerization over racemization. In other words, the inversion of the three-membered ring, in contrast to that of the homofulvenes **2a**, **2b**, and **4**, takes place without the rotation of the alkenylidene group as well. The geometric isomerization is observed without the assistance of the "gear mechanism". Its activation enthalpy (Table 2) is very similar to the racemization barrier of the homofulvenes (Table 3).

Although the racemization is slower than the geometric isomerization (by a factor of 2−3), its activation energy is less. The reason is to be found in the *A* factor, which is

Table 2. Activation parameters

	T_m [°C]	E_a [a] [kcal·mol^{-1}]	log A	$\Delta H^{\ddagger}$[a] [kcal·mol^{-1}]	$\Delta S^{\ddagger}$[a] [cal·K^{-1}·mol^{-1}]
$k_{(+)\text{-}\mathbf{2c},(-)\text{-}\mathbf{2c}}$	167	32.1±0.1	11.84±0.06	31.2±0.1	−7.14±0.28
$k_{(S)\text{-}\mathbf{3c},\mathbf{2c}}$	202	4.8±0.2	12.39±0.12	3.8±0.2	−4.75±0.53
$k_{(+)\text{-}cis\text{-}\mathbf{7},(+)\text{-}trans\text{-}\mathbf{7}}$	196	34.7±0.2	13.06±0.11	33.8±0.2	−1.66±0.50
$k_{(+)\text{-}cis\text{-}\mathbf{7},(-)\text{-}cis\text{-}\mathbf{7}}$	196	32.6±0.4	11.69±0.30	31.6±0.4	−8.04±0.92
$k_{(+)\text{-}cis\text{-}\mathbf{7},(-)\text{-}trans\text{-}\mathbf{7}}$	196	32.7±0.4	11.69±0.30	31.7±0.4	−8.00±0.90
$k_{(Z)\text{-}\mathbf{17},(E)\text{-}\mathbf{17}}$	211	32.4±0.3	11.86±0.15	31.4±0.3	−7.24±0.66
$k_{(E)\text{-}\mathbf{17},\mathbf{19}}$	165	32.1±0.5	11.98±0.27	31.2±0.5	−6.45±1.23
$k_{\mathbf{19},(E)\text{-}\mathbf{17}}$	165	6.8±0.1	13.47±0.04	5.9±0.1	0.33±0.15
$k_{exo\text{-}\mathbf{37},endo\text{-}\mathbf{37}}$	101	30.6±0.9	14.07±54	29.8±0.9	14.25±10.34
$k_{endo\text{-}\mathbf{37},exo\text{-}\mathbf{37}}$	101	30.0±0.8	13.78±0.50	29.2±0.8	8.69±9.57
$k_{(E)\text{-}\mathbf{40},(Z)\text{-}\mathbf{40}}$ (hexane)	120	28.5±0.3	11.98±0.15	27.7±0.3	−6.30±0.32
$k_{(Z)\text{-}\mathbf{40},(E)\text{-}\mathbf{40}}$ (hexane)	120	28.4±0.3	11.93±0.15	27.6±0.3	−6.49±0.66
$k_{\mathbf{40},\mathbf{41s}}$	127	29.7±0.2	12.88±0.10	28.9±0.2	−2.18±0.46
$k_{\mathbf{41s},\mathbf{40}}$	127	10.1±0.3	12.99±0.17	9.3±0.3	−1.35±0.42
$k_{41s,41t}$[b]	127	0.0±0.1	7.64	−	−
$k_{41t,41s}$[b]	127	2.8±0.3	8.25	−	−
$k_{\mathbf{41s},\mathbf{46}}$	127	11.3±0.3	11.96±0.17	10.5±0.3	−6.38±0.76
$k_{\mathbf{41s},\mathbf{47}}$	127	11.3±0.3	12.01±0.16	10.5±0.3	−6.16±0.72
$k_{\mathbf{41s},\mathbf{48}}$	127	11.1±0.1	12.10±0.09	10.3±0.1	−5.74±0.40
$k_{\mathbf{48},\mathbf{49}}$	127	27.9±0.2	11.09±0.09	27.1±0.2	−10.39±0.42

[a] Uncertainty limits are based on a 95% confidence level and were calculated for data obtained by simulation by the method of Nelder.[35] − [b] No uncertainty limit for A factor (see text).

smaller by more than one order of magnitude (Table 2). Hence, **12** cannot be formed by way of **13**. The activation energy for the racemization of **7** (E_a = 32.6 kcal·mol^{-1}) is considerably smaller than that for the equally stabilized phenylmethylallene (42.3 kcal·mol^{-1} [7]), indicating that the racemization of **7** is assisted by the opening of the cyclopropane ring. The racemization is therefore a truly concerted reaction.

Table 3. Calculated values [kcal·mol^{-1}] for the diradical wells of the homofulvenes **2a**−**d**

2	**a**	**b**	**c**	**d**
ΔH_f^0(**2**)[13]	52.9	83.2	32.5	44.2
$\Delta H^{\ddagger}$(rac.)[3]	34.6	33.6	31.2	34.4
ΔH_f^0(TS)	87.5	116.8	63.7	78.6
ΔH_f^0[(*S*)-(**3**)][14]	85.2	106.4	61.6	75.0
$\Delta\Delta H$(gap)	2.3	10.4	3.8 exp. 2.1 calcd.	3.6

The preferred formation of the product formed with simultaneous inversion of the cyclopropane ring and of the double bond, as seen for the homofulvenes **2** and **4**, is no longer observed for the alkenylidene derivative. Starting from (+)-*cis*-**7**, the isomers (−)-*cis*-**7** and (−)-*trans*-**7** are formed in practically equal concentrations (for the rate constants for this transformation see Table 4).

4. Enthalpy Well of the Orthogonal Diradical 3

In the case of homofulvene isomerization, we had postulated a two-step mechanism involving the orthogonal diradical **3** as the intermediate. With the goal of demonstrating

Table 4. First order rate constants for the rearrangement of (+)-*cis*-**7**

Temp. [°C]	$k_{(+)\text{-}cis\text{-}\mathbf{7},(+)\text{-}trans\text{-}\mathbf{7}^{\bullet}}$ 10^4 [s^{-1}]	$k_{(+)\text{-}cis\text{-}\mathbf{7},(-)\text{-}cis\text{-}\mathbf{7}^{\bullet}}$ 10^4 [s^{-1}]	$k_{(+)\text{-}cis\text{-}\mathbf{7},(-)\text{-}trans\text{-}\mathbf{7}^{\bullet}}$ 10^4 [s^{-1}]
171.35	1.0372	0.4453	0.5610
182.10	2.4519	1.0488	1.2884
191.55	5.6011	2.1636	2.5691
201.60	11.901	4.8232	5.3260
211.60	26.319	10.124	10.770
221.80	53.221	18.971	22.795

that **3** is indeed a true intermediate, trapping experiments were performed. However, attempts to characterize this diradical by oxygen trapping failed when dimethylhomofulvene **2d** was used as the substrate. A competing isomerization, yielding isopropylbenzene, took place[8] at temperatures > 230 °C. In order to suppress this rearrangement we chose the tetramethyl derivative **2c** as the substrate in this work. Compound **2c** is accessible by addition of diazopropane to dimethylfulvene (**14**) and photolysis of the adduct **15** (Scheme 6).

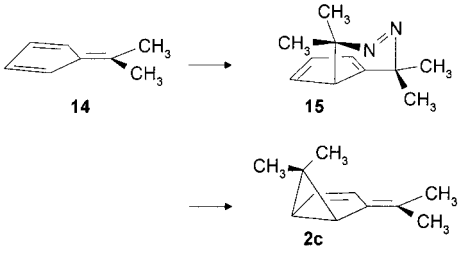

Scheme 6. Synthesis of **2c**

Separation of the enantiomers was achieved by HPLC through a triacetylcellulose column, yielding (+)- and (−)-**2c** in *ee*s of 99.8%. The racemization rate of **2c** was measured in *n*-hexane at six temperatures (142−190 °C), using a Chiralcel OD-H column (Baker) for analysis of the reaction. The resulting activation parameters are listed in Table 2 and are based on the first-order rate constants given in Table 5.

Table 5. Racemization rate (+)-**2c** ⇄ (−)-**2c**

Temp. [°C]	$k_{(+)\text{-}\mathbf{2c},(-)\text{-}\mathbf{2c}}\cdot10^5$ [s^{-1}]
141.60	0.8352
151.70	2.0402
161.90	5.0262
172.00	11.641
182.10	26.501
192.70	59.197

The activation enthalpy for the racemization ($\Delta H^{\ddagger}$ = 31.1 kcal·mol^{-1}) is 3.3 kcal·mol^{-1} lower than that for the analogous reaction of **2d**.[1] This difference is comparable to the substituent effects from the geminal dimethyl group observed for other cyclopropane derivatives,[9,10] and can be attributed to ground-state destabilization of the three-membered ring by the methyl groups.[9]

Information concerning the enthalpy well of the orthogonal diradical **3c**, an intermediate in the racemization, was obtained by the gas-phase thermolysis of **2c** in the presence of oxygen. The substrate, which is nearly stable ($k_{dis} \approx 5.0\cdot10^{-6}$ s^{-1}) in the absence of oxygen at temperatures of 200 °C, now disappears following a pseudo first-order rate law. No new products were detectable by GC. We interpreted the loss of mass as the trapping of the diradical **3c** and determined its rate at six temperatures and three oxygen pressures (0−1000 mbar).

As shown in Figure 1, the oxygen-dependence of the trapping rate up to a pressure of 1 bar is a linear function of the oxygen concentration. Though the blind value mentioned above prevented analysis at very low oxygen concentrations and hence the determination of the singlet−triplet splitting of the diradical, the slope of the curve in Figure 9 is most probably due to the trapping of the singlet diradical, because of the high concentration of the trapping agent that was used.

For appraisal of the trapping experiments we used the reactions formulated in Scheme 7. Assuming that the trapped intermediate is formed in a preequilibrium, the rate of disappearance of substrate should be given by Equation (1). From this, the desired recombination rate ($k_{\mathbf{3c,2c}}$) of the diradical can be obtained only if the rate constant k_s for the reaction between the diradical and oxygen is known. In agreement with other diradical reactions, we assumed a collision-controlled rate[11] and $k_{\mathbf{2c,3c}}$ to be twice the value of the racemization rate.

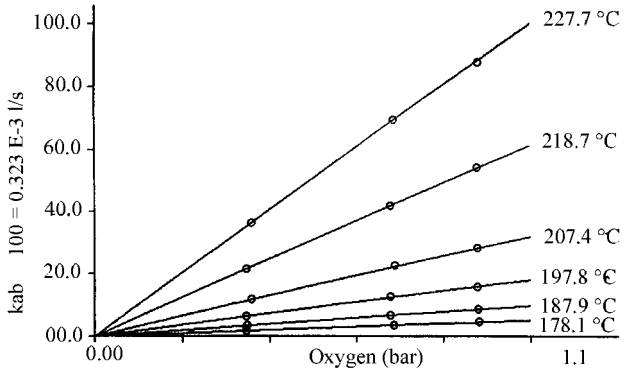

Figure 1. Oxygen dependence of the trapping rate of **3c**

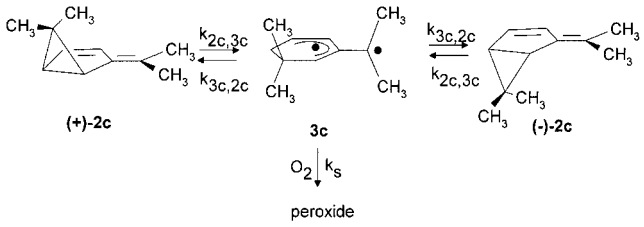

Scheme 7. Mechanism of the trapping reaction of **2c**

$$k_{ab} = k_{\mathbf{2c,3c}}\cdot[1 - k_{\mathbf{2c,3c}}/(k_{\mathbf{2c,3c}} + k_S\cdot[O_2])]\cdot s^{-1} \quad (1)$$

Values for the rate constants $k_{\mathbf{3c,2c}}$ (Table 7) were obtained by simulation of the reactions formulated in Scheme 7 and fitting them to the rate data in Table 6. The resulting activation parameters are listed in Table 2.

Table 6. Rates of disappearance in the thermolysis of **2c** in the presence of oxygen

Temp. [°C]	O_2 [mbar]	$k_{dis}\cdot10^4$ [s^{-1}]
178.10	381.4	0.0606
	755.1	0.1188
	972.3	0.1508
187.90	383.6	0.1173
	747.2	0.2249
	968.8	0.2903
197.80	381.1	0.2208
	747.8	0.4117
	967.6	0.5465
207.40	395.6	0.4147
	757.0	0.7338
	967.2	0.9456
218.70	382.1	0.7285
	747.2	1.411
	967.9	1.663
227.70	394.8	1.292
	756.3	2.466
	968.2	2.838

By using a force-field[11] value for the heat of formation of **2c** [ΔH_f^0(**2c**) = 32.5 kcal·mol^{-1}] and with the activation enthalpy determined as already described (Table 2), we were

able to construct the reaction profile for the racemization of **2c** (Figure 2). The singlet diradical **3c** is located in an enthalpy well of 3.8 kcal·mol^{-1}, a gap comparable to the well of other orthogonal diradicals of the trimethylenemethane type.[1]

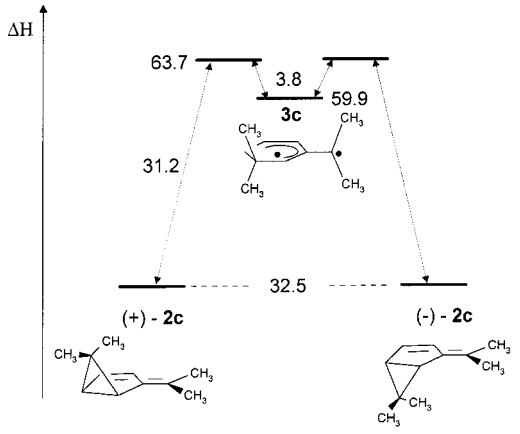

Figure 2. Reaction profile [kcal·mol^{-1}] for the racemization of **2c**

As demonstrated earlier,[1,11] the heats of formation of orthogonal diradicals of the trimethylenemethane type in their triplet states correspond to the values expected for diradicals that do not interact. From this, the heat of formation for **3c** should be accessible from the abstraction of hydrogen from 2-isopropyl-6,6-dimethylcyclohexadieneyl (**16**). As shown in Scheme 8, a value of ΔH_f^0(**3c**) = 60.1 kcal·mol^{-1} is obtained for **3c** in its triplet state, using a force-field[13] value for the heat of formation of the cyclohexadienyl radical **16**.

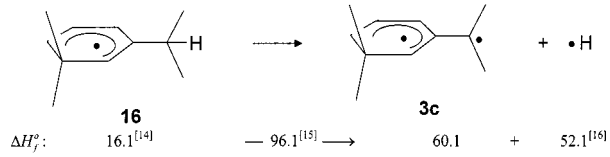

Scheme 8. Expectation value for the heat of formation [kcal·mol^{-1}] of **3c**

The MMEVBH force field[13] gives a calculated heat of formation of ΔH_f^0(**3c**) = 61.6 kcal·mol^{-1} for the singlet state of **3c**, and a negligibly smaller value for the triplet state [ΔH_f^0(**3c**) = 61.2 kcal·mol^{-1}]. This is close to the estimate of 60.1 kcal·mol^{-1} and the experimentally determined value of 59.9 kcal·mol^{-1} (Figure 2).

Table 7. Rates of recombination of **3c** → **2c**

Temp. [°C]	$k_{\mathbf{3c,2c}}\cdot10^{-11}$ [s^{-1}]
178.10	0.1205
187.90	0.1292
197.80	0.1430
207.40	0.1599
218.70	0.1827
227.70	0.2024

For the planar geometry of the diradical **3c** we calculated a heat of formation of 73.5 kcal·mol^{-1} for the singlet state using the MMEVBH force field.[13] This value is substantially higher than the experimentally determined heat of formation [ΔH_f^0(**3c**) = 63.7 kcal·mol^{-1}] for the transition state preceding the diradical. The ring opening producing the orthogonal diradical therefore has to proceed in a concerted fashion with respect to the energetics as well.

By using force-field values for the heats of formation of the homofulvenes **2a**−**d** and experimental activation enthalpies for their racemization, the heats of formation for their respective transition states may be obtained (Table 3). If these values are compared with the calculated heats of formations (MMEVBH force field[13]) for the diradicals **3a**−**d**, a difference of 2−4 kcal·mol^{-1} is observed; this represents the expectation value for the respective diradical well. For **2b**, however, the difference rises to 10.4 kcal·mol^{-1}. This has its cause in the conjugative stabilization of the orthogonal radical by the phenyl group. This stabilization of **3b** is reflected in the lowering of the corresponding transition state by 1 kcal·mol^{-1}, using the barriers of **2a** and **2d** as references (33.6 vs. 34.6 and 34.4 kcal·mol^{-1}). Though this picture is compatible with a concerted opening of the ring, it shows that the transition state is situated early on the reaction coordinate.

5. 2-Benzylidene-3,3-dimethyl-4-methylenebicyclo[3.1.0]hexane (17)

The observation that the ring inversion of the homofulvenes is associated with the rotation of the exocyclic double bond raises the question of the structural spread of this concerted reaction. A molecule that comes close to the geometry of the homofulvenes is 2-benzylidene-3,3-dimethyl-4-methylenebicyclo[3.1.0]hexane (**17**). The cyclopropane ring and the exocyclic double bond are arranged in exactly the same way. Moreover, the same steric interaction between the exocyclic double bond substituent and the tertiary hydrogen atom of the cyclopropane ring is to be expected. Now the thermodynamic driving force for rotation of the exocyclic double bond is no longer the trimethylenemethane structure of the diradical, but the lessening of steric energy by the isomerization (*Z*)-**17** ⇄ (*E*)-**17**.

The synthesis of **17** was achieved by means of a modified Wittig reaction, using the ketone **18**[14] as substrate (Scheme 9). The only product was (*E*)-**17**, which could be equilibrated with (*Z*)-**17** photochemically. The separation of both isomers into their enantiomers was achieved by HPLC; *ee* values of 100% were obtained with a Chiralcel OD-H column (Baker).

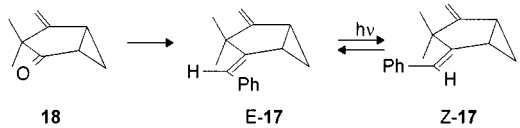

Scheme 9. Synthesis of **17**

Thermolysis of (*Z*)-**17** resulted in the formation of (*E*)-**17** at temperatures of 200 °C. From the equilibrium constant K(*E*-**17**/*Z*-**17**) ≈ 1000, a ΔG of ca. −6.5 kcal·mol^{-1} could be estimated. This is in agreement with the enthalpy difference of −4.9 kcal·mol^{-1} derived by force-field[13] calculations. The rate of the reaction was determined at seven temperatures (180−240 °C). The first-order rate constants are listed in Table 8, and the resulting activation parameters in Table 2.

Table 8. Rates of rearrangement for (*Z*)-**17** → (*E*)-**17**

Temp. [°C]	$K_{(Z)\text{-}17,(E)\text{-}17}$·10^4 [s^{-1}]
181.50	1.8862
191.60	4.2239
201.60	8.8711
211.70	17.747
221.70	33.176
231.90	66.512
242.10	135.55

Starting from one of the pure enantiomers of (*Z*)-**17**, the enantiomers of (*E*)-**17** were formed in exactly a 1:1 ratio; racemization of the starting material is competing with geometric isomerization. By extrapolation of the composition of the product material we determined the rate ratio of isomerization relative to racemization to be nearly 1:1 (200 °C).

The formation of the racemic rearrangement products (*E*)-**17** in the thermolysis of (+)-(*Z*)-**17** requires an achiral intermediate. For a concerted reaction, an unequal population of the chiral transition states (+)-**20** and (−)-**20** would be required; this does not fit with the observation of racemic products. Initial formation of the planar diradical (*Z*)-**19** seems reasonable, and this may react by competing pathways to give (−)-(*Z*)-**17** or, by way of **20**, (*E*)-**19**.

The subsequent mechanism is formulated in Scheme 10. Convincing support is to be found in the observation that racemization of (*E*)-**17** and of (*Z*)-**17** proceeds at the same rate, although (*E*)-**17** is the thermodynamically more stable isomer. That requires that racemization and geometric isomerization be different processes. A further hint of the multi-step course of the geometric isomerization (*Z*)-**17** ⇄ (*E*)-**17** is the unusual *A* factor (A = 8.7·10^{11} s^{-1}). For a one-step mechanism and a styrene-derived intermediate, one would have expected a value at least one order of magnitude higher.[13]

Additional direct proof of the formation of an intermediate diradical was obtained by trapping experiments, on carrying out the thermolysis of (*E*)-**17** in the presence of oxygen. Supercritical CO_2 was chosen as the reaction medium, since it is possible to achieve oxygen pressures of up to 200 bar under these conditions.[15] The substrate, which had been stable in the absence of oxygen at temperatures about 180 °C ($k_{dis} < 10^{-6}$ s^{-1}), now disappeared according to pseudo first-order kinetics. No products of low molecular mass were formed. The rate of the reaction (Table 9) was measured at four temperatures (150−180 °C) and up to seven oxygen concentrations (0−180 bar).

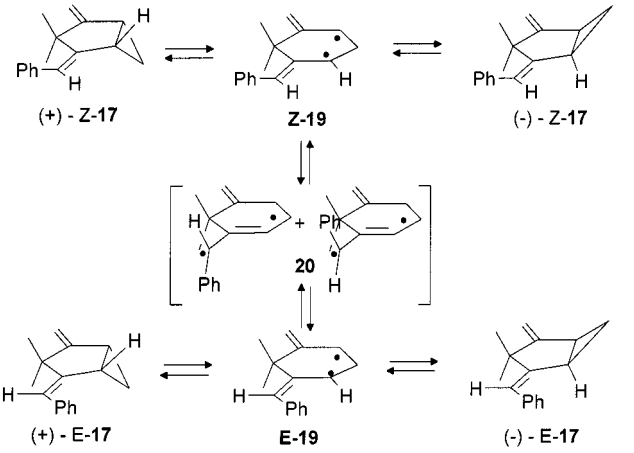

Scheme 10. Mechanism of the isomerization of (*Z*)-**17** ⇄ (*E*)-**17**

Table 9. Rates of disappearance in the thermolysis of (*E*)-**17** in the presence of oxygen

Temp. [°C]	O_2 [bar]	k_{dis}·10^4 [s^{-1}]
150.7	63.9	0.1759
	111.8	0.2065
	179.5	0.2270
160.4	0.0	0.0365
	71.1	0.3845
	119.7	0.4529
	180.3	0.4973
170.5	0.0	0.0291
	31.0	0.5077
	60.3	0.7270
	91.5	0.8653
	119.8	0.9485
	151.4	1.015
	181.9	1.062
180.3	30.6	0.9316
	72.8	1.543
	121.9	1.910
	181.3	2.159

For numerical assessment of the trapping experiments we used the reactions formulated in Scheme 11. The oxygen dependence of the trapping rate (Figure 3) is nonlinear, as is to be expected for the trapping of an intermediate formed in a preequilibrium [Equation (1)]. In contrast to the trapping of **3c**, the approach of the trapping rate to the limiting plateau value can be observed in this case due to the high oxygen pressure. When the plateau is reached, all intermediates are intercepted and the trapping rate becomes identical to $k_{(E)\text{-}17,(E)\text{-}19}$. As usual, k_s was equated to the rate of a collision-controlled reaction.[11] The activation parameters derived by simulation of Scheme 11 and fitting to the data in Table 9 are listed in Table 2.

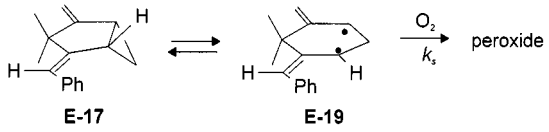

Scheme 11. Mechanism of the trapping reaction of (*E*)-**17**

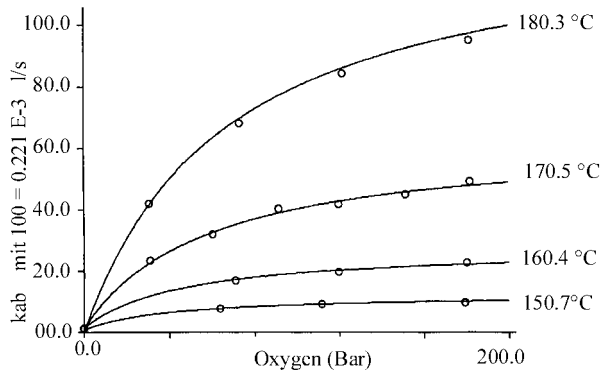

Figure 3. Oxygen-dependence of the trapping rate of (*E*)-**19**

The use of force-field[13] values for the heats of formation of the geometric isomers, in addition to the experimental activation parameters determined above, enabled us to construct the reaction profile for the equilibrium (*Z*)-**17** ⇄ (*E*)-**17** (Figure 4). It was assumed that (*E*)-**19** and (*Z*)-**19** were protected by equivalent enthalpy barriers.

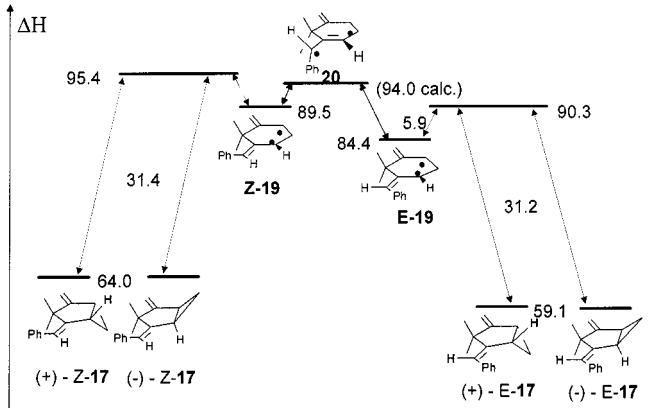

Figure 4. Enthalpy profile [kcal·mol^{-1}] for the equilibrium (*E*)-**17** ⇄ (*Z*)-**17**

6. 6-Methylenebicyclo[3.1.0]hex-2-ene (21)

The diradical **3**, formed in the thermolysis of homofulvene, was considered to be similarly accessible by thermolysis of **21**. Two possibilities also exist for this process: Firstly a concerted reaction proceeding directly to the thermodynamically more stable orthogonal diradical, and secondly a two-step reaction involving the energetically less favorable, planar diradical in an initial step.

The synthesis of **21** had already been unsuccessfully attempted by Berson.[16] However, its preparation proved to be possible when the alcohol obtained from ketone **22** after its conversion into the selenide **23** was oxidized by H_2O_2 at −20 °C (Scheme 12). Unfortunately, **21** rearranges even at 0 °C, yielding the homofulvene **2e**, and so it is not an appropriate substrate for stereochemical analysis. Stable derivatives of **21** have been found by Berson[16] and Brune,[17] in the preparation of the acetal **24** and the substitution products **25a** and **25b**.

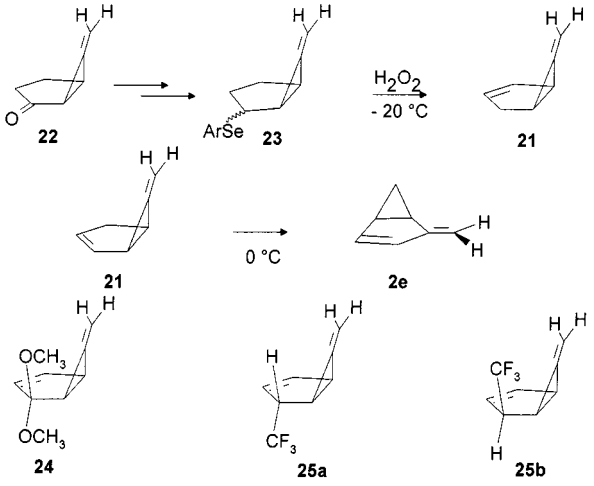

Scheme 12. Synthesis and rearrangement of **21**

We avoided the troublesome rearrangement of **21** by using the benzo derivative. The synthesis of the required butenylidene compound **26** was achieved by addition of the respective vinylidenecarbene to indene **27**, applying the method of Stang[18] (Scheme 13). The separation of (*E*)-**26** and (*Z*)-**26** into their enantiomers was performed by HPLC using a Chiralcel OD-H column (Baker), yielding the isomers each in 100% *ee*.

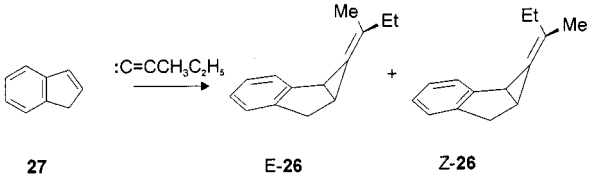

Scheme 13. Synthesis of **26**

Thermolysis both of (+)-(*Z*)-**26** and of (+)-(*E*)-**26** at 70 °C again resulted in the geometric isomerization and racemization of the starting materials. The enantiomer of the starting compound and the two enantiomers of the rearranged products were formed in a ratio of 1:1:1. The analysis was performed by HPLC, using a Chiralcel OD-H column (Baker), conditions that allowed baseline separation of all four isomers. The situation is different from the homofulvene isomerization, since the products were in that case formed in varying concentrations. The observation of a 1:1:1 ratio of the reaction products in the thermolysis of **26** is possible only if the formation of a racemic mixture of the orthogonal diradical **29** is considerably faster than the racemization of the substrate (Scheme 14). On one hand, this condition could be achieved by rotation of the initially formed planar diradical **28** being much faster than its recombination to yield **26**. On the other hand, the reaction products would also be generated in the same observed ratio by direct formation of the racemic mixture of the orthogonal diradicals (*S*)- and (*R*)-**29**. The initial formation of the planar diradical **28**, followed by a fast isomerization to yield the orthogonal diradicals **29**, is surprising if one con-

siders that in the equivalent reaction of **30** (Scheme 15) the rotational barrier **31** ⇄ **32** is higher (2.2 kcal·mol^{-1}) than the recombination barrier **31** ⇄ **30**.[1]

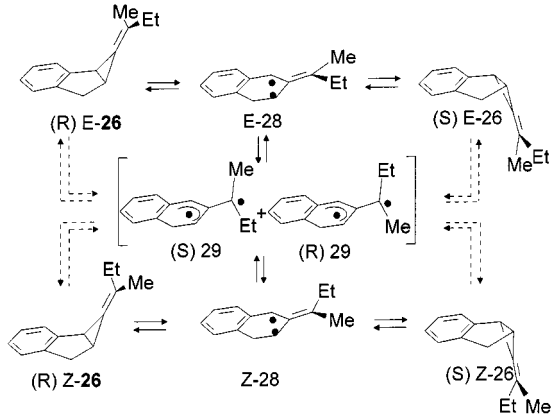

Scheme 14. Thermolysis of **26**

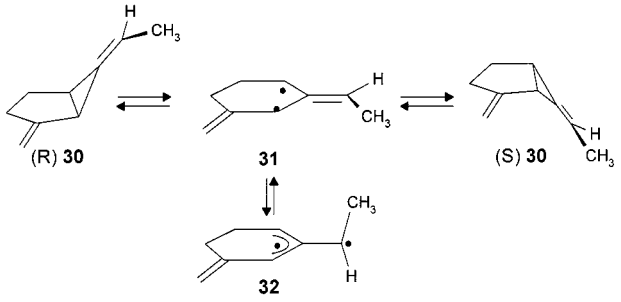

Scheme 15. Thermolysis of **30**

On the other hand, the assumption of the initial formation of the orthogonal diradicals **29** encounters the same obstacle, as the equivalent concerted ring opening had not been observed for **30**. One might argue that the different degree of substitution of the rotating double bond − i.e., the stabilization of the orthogonal diradical **29** − reduces the rotational barrier. But it seems doubtful that this interpretation is sufficient to explain the different behavior of **26** and **30**.

The postulated small barrier for the isomerization **28** ⇄ **29** becomes more acceptable if it is assumed that the barrier **31** ⇄ **32** (2.2 kcal·mol^{-1}) is truly the unusual value. Rotation around an olefinic double bond is a one-step reaction and so the observation of a rotational barrier for the planar trimethylenemethane diradical is surprising in itself. Its observation might be associated with the adjustment of the bond length of the π-system[1] and so might be sensitive to structural changes.

Supporting evidence for this interpretation is to be found in the work of Wegener,[19] who reported that the enthalpy for the rotation **35** ⇄ **36** in the case of 6-ethylidene-3-methylbicyclo[3.1.0]hexane (**33**) was smaller than that for the recombination **35** ⇄ **34** by 2.4 kcal·mol^{-1} (Scheme 16). The close similarity to the isomerization of **26** is obvious. In that case the planar geometry of the primary diradical **35** was also established by oxygen-trapping experiments.[20] The heat of formation of the trapped diradical **35** in its singlet state [ΔH_f^0(**35**) = 78.3 kcal·mol^{-1}] was over 10 kcal·mol^{-1} greater than the force-field[13] value for the orthogonal diradical **36**.

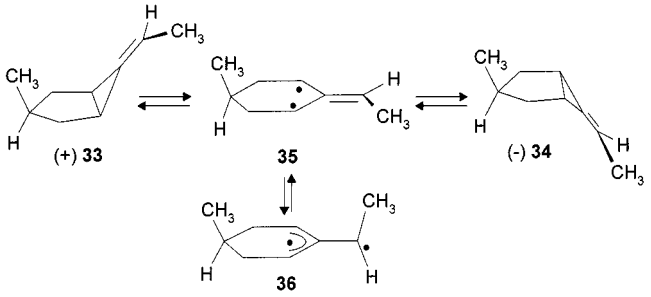

Scheme 16. Thermolysis of **33**

For the homofulvenes, the initial formation of the orthogonal diradicals was derived from the selectivity of the product formation. Conversely, the absent selectivity of **26** implies no unambiguous result. Comparison with the behavior of the other methylenecyclopropanes demonstrates that it is reasonable to assume that the orthogonal diradical **29** is not the primary product. The formation of an achiral intermediate has to occur first, and **28** is this initial intermediate.

The thermolysis of the bicyclic alkenylidene derivatives in analogy to the homofulvenes was also studied.[21] The synthesis of compound **37** was achieved by addition of propenylidene to 1,1-dimethylindene using the method of Hartzler[22] (Scheme 17). After separation of the *exo* and *endo* isomers, the respective enantiomers could be separated by HPLC, using a triacetylcellulose column and providing the isomers in optically pure form.

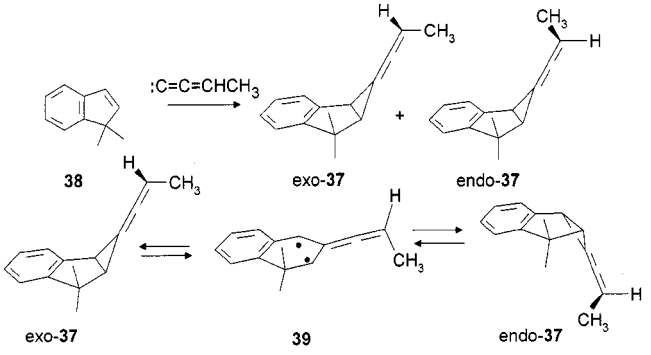

Scheme 17. Synthesis and rearrangement of **37**

Thermolyses of **37** were carried out at six temperatures (80−130 °C) in hexane. For the *exo* ⇄ *endo* isomerization, as the only observable reaction, the first-order rate constants listed in Table 10 were obtained. The resulting activation parameters are presented in Table 2.

Table 10. Rate constants of the equilibrium *exo*-**37** ⇄ *endo*-**37**

Temp. [°C]	$k_{exo\text{-}37,endo\text{-}37}\cdot10^5$ [s^{-1}]	$k_{endo\text{-}37,exo\text{-}37}\cdot10^5$ [s^{-1}]
78.98	1.2136	1.5047
88.91	4.1201	4.7832
98.75	12.672	13.937
108.78	37.528	41.778
118.72	104.18	110.45
127.11	237.12	254.89

Thermolysis of either pure enantiomer gives rise to the formation of only one enantiomer of the geometric isomer. Not even long reaction times (2500 s) at 98.9 °C caused racemization. The isomerization must therefore proceed exclusively by way of the "planar" diradical **39**. The concerted reaction, observed with the homofulvene **7**, in which racemization and isomerization take place in one step, does not occur.

7. 7-Benzylidenebicyclo[4.1.0]hept-2-ene (40)

The nonconcerted pathways for the ring opening of the bicyclic methylenecyclopropanes **26**, **30**, **33**, and **37** pose the question of whether it is possible to change the course of these reactions by changing the substituents. With the aim of answering this question we analyzed the stereochemistry of the ring opening of **40**. Here, the orthogonal diradical is strongly stabilized by the phenyl group. This might induce concerted ring opening, resulting in the diradical **41**.

The preparation of **40** was carried out in analogy to a procedure reported by Seebach.[23] After conversion of the dibromocarbene adduct of 1,3-cyclohexadiene (**42**) into its lithium derivative **43**, treatment with benzaldehyde gives the bromoalcohol **44**. Compound **44** was transformed into the corresponding silyl ether **45**, which gave (*Z*)- and (*E*)-**40** by elimination upon treatment with *tert*-butyllithium (Scheme 18). After separation of the isomers it was possible to separate the enantiomers by HPLC, using a triacetylcellulose column and obtaining the enantiomers in 100% *ee*.

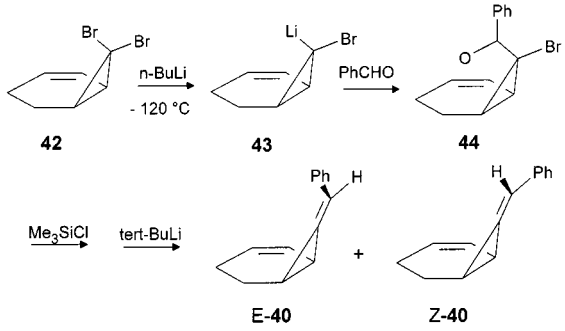

Scheme 18. Synthesis of **40**

Thermolysis of **40** resulted in the geometric isomerization (*E*)-**40** ⇄ (*Z*)-**40**. The first-order rate constants for this reaction were determined in hexane at seven temperatures in the range 90−160 °C (Table 11). Their temperature dependence produced the activation parameters listed in Table 2.

Table 11. First order rate constants for the equilibrium (*Z*)-**40** ⇄ (*E*)-**40**

Temp. [°C]	$k_{(Z)\text{-}40,(E)\text{-}40}\cdot10^4$ [s^{-1}]	$k_{(E)\text{-}40,(Z)\text{-}40}\cdot10^4$ [s^{-1}]
89.42	0.0721	0.0700
89.42	0.0697	0.0683
99.44	0.1764	0.1756
109.38	0.5614	0.5638
109.38	0.5065	0.5098
119.31	1.176	1.205
129.15	3.145	3.063
149.37	19.40	19.29
149.37	18.68	18.84
158.26	36.03	33.75
158.26	36.97	35.79

In parallel with this isomerization, the racemization (*R*)-**40** ⇄ (*S*)-**40** also took place. The ratios of these two competing reaction pathways were determined at 122, 149, and 173 °C. When the starting material was optically pure (+)-(*Z*)-**40**, the three isomers appearing − (−)-(*Z*)-**40** and (+/−)-(*E*)-**40** − were formed in exactly a 1:1:1 ratio. When the starting material was the other isomer, (−)-(*E*)-**40**, the observation was the same, the three isomers appearing were formed in an identical manner, in a 1:1:1 ratio (Table 12). As HPLC analysis using a cellulosetriacetate column permitted monitoring of all four isomers separately in these measurements, the uncertainty of the product composition was reduced to $< 2\%$.

At temperatures above 130 °C these interconversions of **40** were accompanied by the irreversible formation of isomers **46**−**48**, with the latter reacting further to give **49** by electrocyclic ring closure (Scheme 19). Noticeably, the formation of the geometric isomers **46** and **47** is independent of the geometry of their precursor **40**. Starting either from the (*Z*) form or from the (*E*) form results in the same ratio of **46**/**47**.

It is thus reasonable to assume that all products are formed by way of the same intermediate diradical **41**, which is preferentially stabilized by the formation of **40**, but at higher temperatures has the ability to react to give **46**−**48**. The exactly equal rates for racemization and geometric isomerization of **40** practically rule out a planar geometry for **41**. An orthogonal diradical, which would be compatible with this observation, would have to be a racemate. However, this is not compatible with the selectivity observed for the homofulvenes. In order to test the postulated orthogonal geometry of the diradical **41**, we carried out trapping experiments to examine its singlet−triplet splitting, which is a diagnostic criterion for the geometry of trimethylenemethane derivatives.[1]

In addition to the reactions already described, gas-phase thermolysis of **40** in the presence of oxygen results in disappearance of the substrate following pseudo first-order kinetics. Moreover, the rate of formation of the rearrangement products **46**−**48** is retarded.

Table 12. Product ratios in the thermolysis of optically active **40** (100% *ee* each)

Temp. [°C]	Starting material	(+)-(*Z*)-**40** [%]	(−)-(*Z*)-**40** [%]	(−)-(*E*)-**40** [%]	(+)-(*E*)-**40** [%]
122	(+)-(*Z*)-**40**	61.26	13.30	12.84	12.60
	(+)-(*Z*)-**40**	45.03	18.80	18.25	17.92
	(+)-(*Z*)-**40**	25.18	24.15	25.46	25.20
	(−)-(*E*)-**40**	17.77	17.97	47.89	16.37
149	(+)-(*Z*)-**40**	45.51	18.70	17.81	17.99
173	(+)-(*Z*)-**40**	45.55	18.85	17.46	18.14

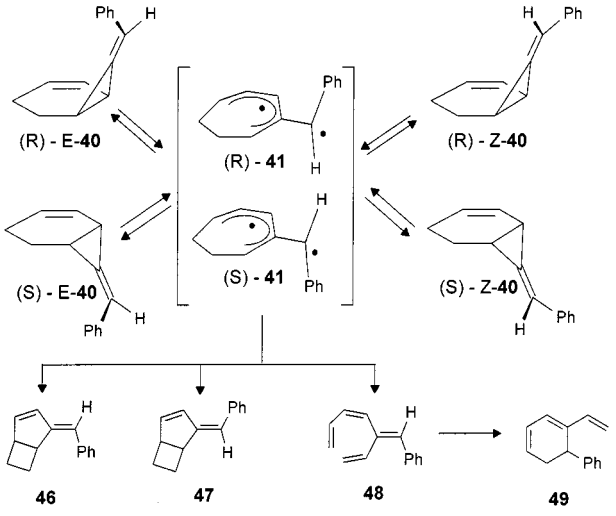

Scheme 19. Thermolysis of **40**

We monitored this reaction at six temperatures (100−150 °C) and up to fourteen oxygen pressures (0−800 mbar). The resulting product distributions are shown in the Supporting Information.

The oxygen-dependence of the trapping rate (Figure 5, top) reveals that the trapping occurs from a preequilibrium. At high oxygen concentrations, the trapping curve asymptotically approaches a limiting value, representing a situation in which the intermediate is trapped quantitatively.

The reasonable assumption that it is actually the intermediate **41** of the interconversion reactions of **40** (Scheme 19) that is trapped is strongly supported by the oxygen dependence of the rearrangement rate (*E*)-**40** $\rightleftarrows$ (*Z*)-**40**. The rearrangement rate slows down with increasing oxygen concentration and approaches zero asymptotically (Figure 5, bottom) in the same manner in which the trapping velocity reaches the twofold interconversion rate under oxygen-free conditions (Figure 5, top). This factor of two [$2\cdot(3.4\cdot10^{-4}\ s^{-1} - 0.7\cdot10^{-4}\ s^{-1}) = 5.4\cdot10^{-4}\ s^{-1}$] can be simply explained as twice the number of reaction pathways in the case of the interconversion [(*E*)-**40**, (*Z*)-**40**] than under oxygen-trapping conditions (peroxide).

The multiplicity of the trapped diradicals can be deduced from the trapping curve at very low oxygen concentrations. As was shown earlier,[24] the slope of the curve is made up of the linear increasing proportion of the trapped singlet diradicals and the decreasing proportion of the triplet diradicals. The latter becomes zero when all triplet diradicals

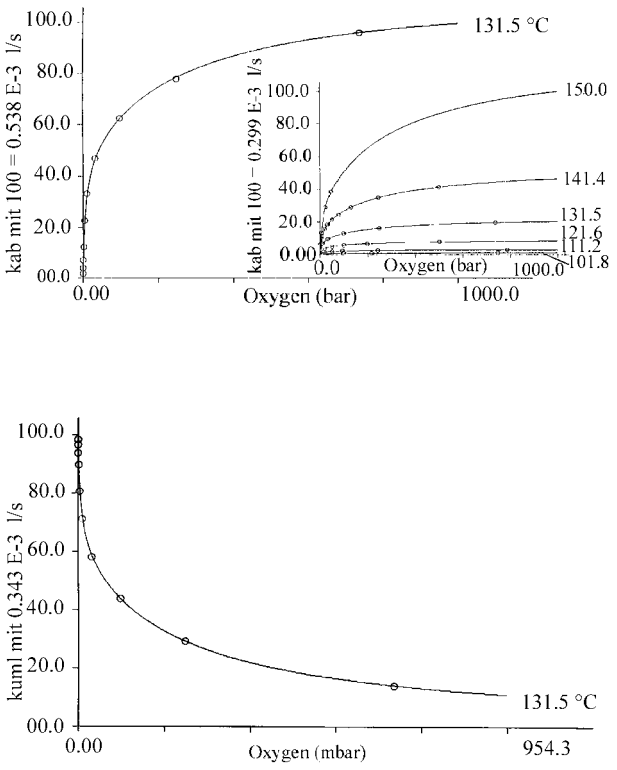

Figure 5. Oxygen-dependence of the rates of disappearance (top) and rearrangement (bottom) of **40**

are exclusively trapped at sufficiently high oxygen concentrations. The outcome is a nonlinear slope at low trapping concentrations, which gradually changes to a linear ascent until the triplet diradicals are trapped quantitatively (Figure 6). The linear branch, its extrapolated intercept with the ordinate, and the nonlinear part of the curve give the rate constants describing the diradical pair.[24] In the case of the diradical **41**, these are $k_{\mathbf{S\text{-}41,40}}$, $k_{\mathbf{S\text{-}41,T\text{-}41}}$, and $k_{\mathbf{T\text{-}41,S\text{-}41}}$.

For evaluation of the trapping experiments, the reaction was simulated according to Scheme 20 and fitted by a simplex routine[6] to the data collected in the Sopprting Information. For the reaction between the diradicals and oxygen, a collision-controlled rate was assumed as usual.[24] The resulting rate constants are listed in Table 13 and the activation parameters derived from their temperature dependence are given in Table 2.

The finding of a singlet-triplet splitting of only 2 kcal·mol^{-1} clearly confirms the orthogonal geometry, al-

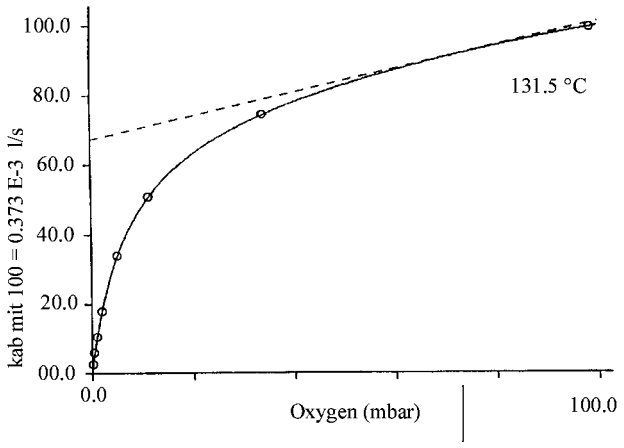

Figure 6. Trapping curve of **40** at 131.5 °C and low oxygen pressures

Table 13. First-order rate constants for the reactions of **40**, **41**, and **48**

Temp. [°C]	101.76	111.28	121.61	131.53	141.41	150.91
$k_{40,41}\cdot10^4$ [s^{-1}]	0.3540	0.9551	2.643	6.910	16.70	35.14
$k_{41,40}\cdot10^7$ [s^{-1}]	1.207	1.736	2.454	3.367	4.545	5.984
$k_{41S,41T}\cdot10^6$ [s^{-1}]	4.349	4.350	4.351	4.353	4.354	4.355
$k_{41T,41S}\cdot10^6$ [s^{-1}]	4.156	4.556	5.017	5.474	5.946	6.415
$k_{41S,46}\cdot10^5$ [s^{-1}]	2.742	4.068	5.536	7.944	11.60	16.14
$k_{41S,47}\cdot10^5$ [s^{-1}]	2.404	3.807	5.588	7.837	10.38	14.40
$k_{41S,48}\cdot10^5$ [s^{-1}]	4.035	6.008	8.800	12.69	16.80	23.08
$k_{48,49}\cdot10^5$ [s^{-1}]	0.6285	1.620	4.261	9.969	23.64	47.89

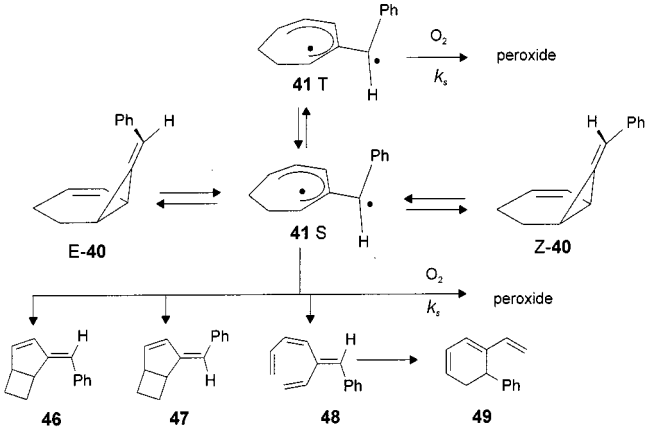

Scheme 20. Mechanism of the trapping reaction of **40**

ready derived from stereochemical arguments, of the trapped diradical. In agreement with previous experiments[1] and with quantum-chemical calculations, the splitting for planar trimethylenemethane diradicals is of the order of 15−20 kcal·mol^{-1}, whereas values of 2−6 kcal·mol^{-1} have been observed for the orthogonal diradical.

The establishing of an orthogonal structure for the intermediate diradical **41** poses a question concerning the concerted nature of the reaction producing this intermediate. In the case of a concerted reaction, diradical **41** and the resulting products should have displayed optical activity, as observed for **3** and **6**, because chiral, optically active starting materials cannot react to produce the racemate of a chiral product by a concerted pathway. Since this is not the case, an achiral intermediate has to be involved, and so **41** is only the subsequent product of a primary, achiral diradical, in analogy with the formation of **29**. The most likely structure for this additional intermediate is the planar diradical **50**, which has to stabilize itself much more quickly as the orthogonal diradical **41**, rather than reacting back to the substrate **40**. Thus, the transition state **50** → **41** should, in analogy to **28**, have a very low barrier. This postulate is indeed expected to be verified because the rotation here is associated with a substantial measure of stabilization. The electron, which in the orthogonal diradical is normally isolated, is now stabilized by the phenyl group, and this should result in a lowering of the rotational barrier according to the Hammond principle.

The resulting heat of formation of the diradical **41** in its triplet state should be equal to the hypothetical value for the molecule with noninteracting radicals. Its heat of formation can be estimated by the abstraction of a hydrogen atom from the benzylic radical **51**. As is shown in Scheme 21, they indeed differ by only 2.1 kcal·mol^{-1}. In Figure 7 the reaction profile of the trapping reaction has been constructed on the basis of a force-field value[13] for the heat of formation of **40** and the experimentally determined activation parameters.

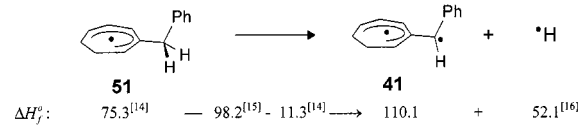

Scheme 21. Calculated values for the heat of formation [kcal·mol^{-1}] of **41**

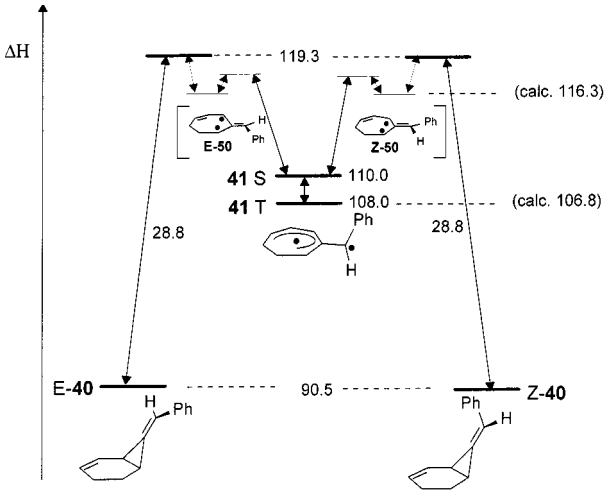

Figure 7. Enthalpy profile [kcal·mol^{-1}] for the trapping reaction of **40**

EVBH force-field calculations for the diradical species agree with the above interpretation as well. The calculated heat of formation for the orthogonal triplet state

[ΔH_f^0(**41**) = 106.8 kcal·mol^{-1}] is close to the experimentally found 108.0 kcal·mol^{-1}.

For the planar diradical, the heat of formation is calculated to be ΔH_f^0(**50**) = 116.3 kcal·mol^{-1} for the singlet state. This is lower in energy than the heat of formation of the transition state producing **50** (119.3 kcal·mol^{-1}).

This situation is completely different to that of the homofulvene **3c**. There, the calculated heat of formation of the singlet state of the planar diradical is much higher than that of the transition state producing **3c**, and thus rules out the intermediate formation of the planar diradical.

8. Discussion

Our understanding of unimolecular reactions is based on the assumption that the vibrational energy of the molecule in the transition state is concentrated in one vibration only. This characterizes the respective transition state[25] and results in the reaction of interest if the activation is sufficient. Whenever more than one bond is broken or formed in a reaction, the individual actions can only take place in one step when the underlying vibrations are coupled. Only under these conditions should a common transition state be possible.

For the bicyclic methylenecyclopropane derivatives (**26**, **30**, **33**, **37**, and **40**) we found that ring opening and rotation of the exocyclic double bond always occur in a stepwise fashion, although the concerted reaction is favored by enthalpy. This observation indicates the low coupling probability of the underlying vibrations. In this sense, the high proportion of least-motion processes in thermal reorganization reactions shows that the coupling of different vibrations of the molecule is more the exception than the rule.

With this in mind, the observation of concerted reaction paths for the isomerization of the homofulvenes **2**, **4**, **7** is of special interest. In contrast to the bicyclic methylenecyclopropane derivatives, ring opening of the cyclopropane and rotation of the exocyclic double bond should proceed here through activation of only one vibration. A high coupling probability for the underlying vibrations has to be postulated.

An alternative explanation for the observed one-step reaction might be the operation of a dynamic gear mechanism. As impressively demonstrated by Mislow,[4] such effects occur only through the interaction of sterically demanding groups. That is not the case with the 7-methylhomofulvenes **2** and **4**. Furthermore, the bond to the exocyclic methylene group has a high double-bond character and the weak steric interactions are not sufficient to overcome the rotational barrier.

There are additional experimental implications ruling out any importance of steric effects in the observed concerted homofulvene isomerization reaction pathway. In passing from the homofulvene **2** to the alkenylidene **7**, in which no steric interactions are possible, the reaction mechanism remains unchanged.

Moreover, electronic effects are not responsible for the concerted reaction. As shown by AM1 calculations,[26] there is no preference for the observed disrotatory ring opening (defined with respect to the C-4−C-5 bond) over its conrotatory counterpart. In any event, orbital-symmetry control is not expected.

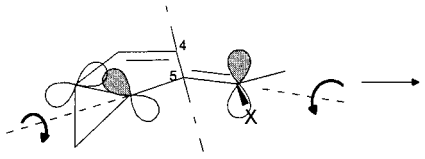

2

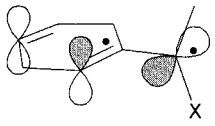

3

What could be the reason for the varying coupling probability of the vibrations responsible for ring opening with rotation of the exocyclic double bond? The different orientations of the axes of the vibrational motion might be an explanation. In the homofulvenes these are oriented nearly parallel, although they are nearly orthogonal in the bicyclic methylenecyclopropanes. It cannot be ruled out that the coupling of the vibrations might also induce a preferred rotational direction of the exocyclic methylene group, causing the observed stereoselectivity.

In agreement with the above reasoning, the homofulvenes **2** and **4** and the alkenylidene **7** react in the same way. Again, the opening of the cyclopropane ring and the rotation of the alkenylidene bond are concerted. In the thermolysis of **7**, however, we observe the generation of the planar diradical **13** rather than to the exclusive formation of the orthogonal diradical **12**. As **13** is the product of cyclopropane ring opening only, there is competition with the concerted reaction channel. This rivalry demonstrates that the two diradicals **13** and **12** have similar thermodynamic properties in this case.

2

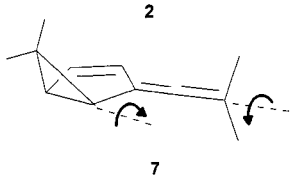

7

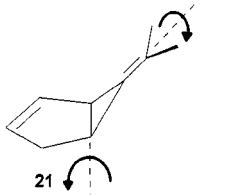

21

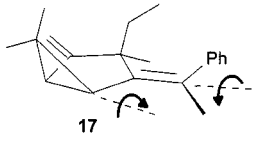

17

According to the interpretation given above, the isomerization of the bis(methylene) compound **17** might also proceed in a concerted fashion. That, however, was not observed. An explanation might be that the concerted reaction channel here is the thermodynamically less favored process,

in spite of the favorable coupling probabilities of the relevant vibrations.

As shown by the thermolysis of **40**, the nonconcerted reaction channel observed for the methylenecyclopropanes cannot be changed just by stabilization of the reaction product. The coupling probability is therefore not determined by the thermodynamics of the product, but by the geometries of the interacting vibrations.

Summing up, we have to conclude that a high coupling probability for the underlying vibrations is a prerequisite for a concerted reaction. As indicated by the homofulvenes, this coupling probability might depend on geometric factors. If a high coupling probability is present, than the likelihood of reacting in a concerted fashion is determined by comparison of its transition state with that of the nonconcerted pathway.

The decomposition of azo compounds is one such example.[3] Here, concerted and nonconcerted decomposition routes are also possible, by activation of the symmetrical or antisymmetrical vibration. The stabilities of the resulting products (or transition states) then dictate which one of the two reaction channels will dominate.

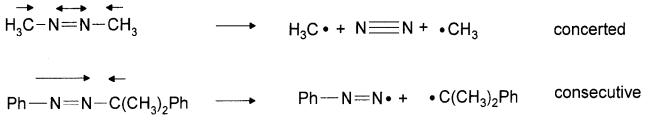

The uncertainty that becomes obvious in assessment of the coupling probabilities of vibrations is an expression of the discrepancy in our knowledge concerning the surfaces of the potential and the free energies. High standards have been achieved for calculation of heats of formation of molecules and intermediates, but only preliminary attempts for judgment of Gibbs energy are available. To establish preferences for concerted or nonconcerted reaction pathways, we have to determine the reaction probabilities, which are given by Gibbs activation energies.

Experimental Section

1. Kinetic Measurements

The rate constants, listed in Tables 4−13, and the Supporting Information were measured by the technique and apparatuses described in the literature.[15,27]

Equipment: ^{1}H and ^{13}C NMR: Bruker AM 400, AM 200. − GC-MS: Hewlett−Packard 5890 A Serie II gas chromatograph (column: OV1, 12.5 m, 0.33 mm) and Hewlett−Packard 5979 Serie MSD mass selective detector. − IR: Perkin−Elmer 681. − Analytical GLC: Intersmat IGC 120 FB, Hewlett−Packard 5890 Series II, nitrogen was used as carrier gas. Preparative GLC: Varian A-90-P3. Integrators: Hewlett−Packard 3390 A, 3395. Analytical HPLC: Spectra-Physics SP5750 Organizer, SP 8700 Solvent Delivery System, Shimadzu SPD-6A Spectrophotometer. Preparative HPLC: Shimadzu LC-8A, Waters Associates Chromatography Pump, Altex Analytical UV Detector + Preparative Analytical Optical Unit, Knauer UV/Vis Filter Photometer.

Preparative Separation of the Enantiomers of 7-Methylhomofulvene (2a): The separation of the enantiomers was achieved by HPLC, starting from a mixture of the geometric isomers. With a triacetylcellulose column and ethanol/water (96:4) as eluent (flow: 1.3 mL/min, UV detector: 254 nm), separation into three peaks, with ratios of 1:2:1 and retention times of 75, 80, and 90 min, was observed. Fractions of the first [(−)-(*E*)-**2a**] and the third [(+)-(*Z*)-**2a**] peak were collected (only the uphill or downhill parts, respectively), and the ethanol solution diluted with water and extracted with pentane. The combined organic layers were dried with Na_2SO_4 and the solvent was removed. Only small quantities of the two isomers could be separated because of the pure separation of the peaks. Use of the pure (*E*) and (*Z*) isomers as starting material did not improve the separation. Optical purities of 92 and 85% *ee*, respectively, were achieved. Analysis was carried out by GC {perpentylated cyclodextrin capillary column, 30 m, 33 °C, hydrogen 1.1 bar, R_t[(−)-(*Z*)-**2a**] = 71 min, R_t[(+)-(*Z*)-**2a**] = 73 min, R_t[(−)-(*E*)-**2a**] = 80 min, R_t[(+)-(*E*)-**2a**] = 83 min}.

11-Methylbenzohomofulvene (4): Ethyltriphenylphosphonium bromide (0.77 g, 2.1 mmol) was dissolved in anhydrous ether (5 mL) under argon. A solution of *n*-butyllithium (15%, commercial solution, 1.6 mol/l in hexane, 1.1 mL, 1.8 mmol) was added, and the solution was stirred for 3 h at room temp. 1a,6a-Dihydro-1*H*-cyclopropa[*a*]inden-6-one (**5**)[5] (0.1 g, 0.69 mmol), dissolved in ether (0.5 mL), was added to the yellow solution of the ylide, and the mixture was stirred for an additional 12 h at room temp. The reaction mixture was hydrolyzed with a small amount of water, the organic layer was concentrated by solvent evaporation, and silica gel chromatography of the residue (pentane) afforded 50 mg of the *cis*/*trans* mixture of the 6-ethylidene-1,1a,6,6a-tetrahydrocyclopropa[*a*]indenes **4** in a ratio of 2.4:1. The assignment of the stereochemistry was achieved by NOE-difference spectroscopy. − MS (70 eV); *m*/*z* (%): 156 (38) [M^+], 141 (100), 128 (22), 115 (24), 102 (4), 76 (7), 63 (8), 51 (7). − ^{1}H NMR (400 MHz, $CDCl_3$): (*Z*)-**4**: δ = 0.37 (q, 1 H), 1.08 (dt, 1 H), 2.03 (d, *J* = 7.3 Hz, 3 H), 2.38 (m, 1 H), 2.55 (m, 1 H), 5.84 (q, *J* = 7.3 Hz, 1 H), 7.10 (m, 2 H), 7.30 (m, 1 H), 7.60 (m, 1 H), (*E*)-**4**: δ = 0.40 (q, 1 H), 1.22 (dt, 1 H), 1.96 (d, *J* = 6.9 Hz, 3 H), 2.55 (m, 2 H), 6.04 (q, *J* = 6.9 Hz, 1 H), 7.10 (m, 2 H), 7.30 (m, 2 H). − One enantiomer of (*E*)-**4** could be separated by preparative HPLC, using a triacetylcellulose column with ethanol/water (96:4) as the eluent (flow: 2.4 mL/min, UV detector: 254 nm), R_t[(−)-(*E*)-**4**] = 65 min, R_t[(+)-(*E*)-**4**] = 70 min, R_t[(+)/(−)-(*Z*)-**4**] = 80 min. Only the uphill flank of the first peak was collected, yielding (−)-(*E*)-**4** in 95% *ee*.

6-Propenylidenebicyclo[3.1.0]hexan-3-ol (9): Potassium *tert*-butoxide (12 g, 0.09 mol) was dissolved in cyclopenten-3-ol (**8**)[27] (50 mL, 0.59 mol) under argon and the solution was cooled to 0 °C. Over 4 h, 3-bromo-1-butyne (8 g, 0.06 mol) was added at 0 °C to the stirred solution. The solution was allowed to warm to room temp. and stirred for an additional 12 h. The reaction mixture was poured onto 800 mL of ice and extracted with ether. The combined organic layers were dried with $MgSO_4$, and the solvent and the excess cyclopentenol were removed by distillation (30 Torr, 60−65 °C). The residue was separated by vacuum distillation (20 Torr), yielding two fractions, a light yellow liquid at 110−120 °C and a white solid at 120−125 °C. Each fraction comprised two of the four 6-propenylidenebicyclo[3.1.0]hexan-3-ol (**9**) isomers (15%). − MS (both fractions); *m*/*z* (%): 136 (3) [M^+], 135 (4), 121 (24), 107 (15), 93 (15), 91 (100), 79 (50), 77 (49), 65 (20), 51 (21), 39 (33). − Liquid fraction (*endo*/*exo* mixture): ^{1}H NMR ($CDCl_3$, 80 MHz): δ = 1.60 (two d, 3 H, CH_3), 1.65−2.2 (m, 7 H), 3.0−4.2 (m, 1 H, CHOH), 4.9−5.4 (m, 1 H, allene-H). − IR (neat): $\tilde{\nu}$ = 3570 cm^{-1}(s), 3200−3500 (broad, s), 3020 (m), 2910−2960 (s), 2850 (m),

2000 (s), 1440 (m), 1410 (w), 1370 (m), 1290 (m), 1210 (m), 1180 (m), 1070 (s), 960 (m), 910 (m), 830 (m) 760 (m). − Solid fraction (*endo* and *exo* mixture): ^{1}H NMR ($CDCl_3$, 80 MHz): δ = 1.45 (broad s, 1 H, OH), 1.67 (d, 3 H, CH_3), 1.55−1.9 (m, 2 H, cyclopropane), 2.0−2.5 (m, 4 H), 4.0−4.3 (m, 1 H, CHOH), 5.0−5.3 (m, 1 H, allene-H). − IR (KBr disk): $\tilde{\nu}$ = 3200−3600 cm^{-1} (m), 3060 (m), 2920−2970 (s), 2850 (m), 2000 (w), 1600 (m), 1450 (m), 1360 (s), 1190 (s), 1180 (s), 1070 (s), 970 (m), 920 (m), 870 (m), 820 (m).

3-(2-Nitrophenylselanyl)-6-propenylidenebicyclo[3.1.0]-hexane (10): 2-Nitrophenylselenocyanate (0.73 g, 3.2 mmol) and 6-propenylidenebicyclo[3.1.0]hexan-3-ol (**9**) (0.22 g, 1.6 mmol) were dissolved in a mixture of anhydrous THF (4 mL) and pyridine (4 mL). Tri-*n*-butylphosphane (0.65 g, 3.2 mmol) was added. The reaction mixture was stirred for 12 h and then concentrated using a rotary evaporator. The residue was used immediately for the elimination procedure.

4-Propenylidenebicyclo[3.1.0]hex-2-ene (7): The residue from the above selenide preparation of **10** was dissolved in chloroform (5 mL) and the solution was cooled to 0 °C. Pyridine (100 μL) and an aqueous hydrogen peroxide solution (30%, 500 μL, 4.4 mmol H_2O_2) were added. The reaction mixture was stirred for 1 h at 0 °C and an additional 3 h at room temp. and then concentrated using a rotary evaporator. The residue was dissolved in pentane and washed with water. After evaporation of the solvent, silica gel chromatography of the residue (pentane) afforded a mixture of *cis*- and *trans*-4-propenylidenebicyclo[3.1.0]hex-2-ene (**7**). Further purification was achieved by preparative GC (DC 200, 20%, 0.5 m 70 °C, R_t = 13 min, both isomers). − MS (70 eV); *m*/*z* (%): 118 (45) [M$^+$], 117 (100), 115 (75), 103 (25), 91 (55), 78 (64). − IR (neat): $\tilde{\nu}$ = 3120 cm^{-1} (w), 3060 (s), 2900−3000 (s), 2850 (s), 1950 (m), 1660 (w), 1560 (m), 1440 (s), 1370 (m), 1340 (m), 1310 (w), 1280 (w), 1200 (s), 1170 (s), 1020 (s), 800 (s), 750 (s), 720 (s) cm^{-1}. − ^{1}H NMR (200 MHz, C_6D_6): δ = 0.72 (m, 1 H), 0.45 (m, 1 H), 1.60 (2 d, *cis*/*trans*, 3 H), 1.90 (m, 1 H), 2.22 (m, 1 H), 5.25 and 5.45 (m, both peaks 1 H, *cis*/*trans*), 5.82 (m, 2 H). − Separation of the enantiomers was achieved by HPLC, using a triacetylcellulose column and ethanol/water (96:4) as eluent (flow 0.8 mL/min), R_t[(+)-**A**] = 132 min, R_t[(−)-**A**] = 141 min, R_t[(+)/(−)-**B**] = 150−160 min. Only the uphill flank of the first peak was collected, because of the poor separation. It yielded (+)-**A** in 97% *ee*. The stereochemistry of this product was not determined.

Cycloaddition between 6,6-Dimethylfulvene (14) and 2-Diazopropane: 6,6-Dimethylfulvene (**14**)[29] (1.5 g, 14 mmol) was added to a cold solution of 2-diazopropane in ether. The reaction mixture was allowed to warm to room temp. and stirred for an additional 12 h. After evaporation of the solvent, silica gel chromatography of the residue (pentane) afforded three fractions, excess 6,6-dimethylfulvene (**14**), the [2,3]-addition product 1,1,4,4-tetramethyl-2,3-diazaspiro[4.4]nona-2,6,8-triene, and a mixture of the two dihydrocyclopentapyridazines formed by dipolar [6,3]-cycloaddition (1,1,4,4-tetramethyl-4,4a-dihydro-1*H*-cyclopenta[*d*]pyridazine and 3,3,4,4-tetramethyl-4,7a-dihydro-3*H*-cyclopenta[*c*]pyridazine). − 1,1,4,4-Tetramethyl-2,3-diazaspiro[4.4]nona-2,6,8-triene: MS (70 eV); *m*/*z* (%): 148 (1) [M$^+$], 133 (70), 115 (8), 105 (100), 90 (57), 77 (21), 65 (20), 51 (19), 41 (66) − ^{1}H NMR (200 MHz, $CDCl_3$): δ = 1.38 (s, 12 H), 6.15 (m, 2 H), 6.22 (m, 2 H). − Mixture of the two dihydrocyclopentapyridazines: MS (70 eV); *m*/*z* (%): 148 (14) [M$^+$], 133 (100), 115 (13), 105 (95), 91 (50), 77 (23), 65 (18), 51 (15), 41 (44). − ^{1}H NMR (200 MHz, $CDCl_3$): δ = 1.10 (s, 3 H), 1.28 (s, 3 H), 1.49 (s, 3 H), 1.58 (s, 3 H), 1.82 (s, 3 H), 1.85 (s, 3 H), 1.92 (s, 3 H), 2.24 (s, 3 H), 2.76 (d, 1 H), 2.86 (d, 1 H), 5.65 (d, 1 H), 5.72 (d, 1 H), 6.00 (d, 1 H), 6.23 (m, 2 H), 6.35 (m, 1 H). − IR (neat): $\tilde{\nu}$ = 3030 cm^{-1}, 2970, 2920, 2910, 1665, 1575, 1555, 1460, 1445, 1380, 1375, 1360, 1255, 1235, 1140, 1130, 1090, 1035, 905, 885, 780, 750.

6,6,7,7-Tetramethylhomofulvene (2c): The mixture of the two dihydrocyclopentapyridazines (0.5 g) was dissolved in hexane (5 mL) and irradiated (Rayonet reactor) for 2 h at 254 nm. After evaporation of the solvent, silica gel chromatography of the residue (pentane) afforded 0.2 g of 6,6,7,7-tetramethylhomofulvene **2c**. − MS (70 eV); *m*/*z* (%): 148 (14) [M$^+$], 133 (84), 115 (15), 105 (100), 91 (56), 77 (28), 65 (22), 51 (19), 41 (53). − ^{1}H NMR (200 MHz, $CDCl_3$): δ = 1.06 (s, 3 H), 1.18 (s, 3 H), 1.84 (s, 3 H), 1.87 (s, 3 H), 2.10 (s, 2 H), 5.98 (m, 1 H), 6.35 (d, 1 H). − ^{13}C NMR (200 MHz, $CDCl_3$): δ = 14.4, 21.0, 22.0, 26.9, 27.2, 34.3, 39.0, 125.5, 131.2, 133.1, 139.3. − IR (neat): $\tilde{\nu}$ = 3050 cm^{-1}, 3020, 2980, 2940, 2910, 2860, 2730, 1660, 1560, 1450, 1375, 1360, 1295, 1160, 1125, 1005, 980, 875, 825, 765, 745. − Separation of the enantiomers was achieved by HPLC, using a triacetylcellulose column and ethanol/water (96:4) as the eluent (UV detector: 254 nm, flow: 1.5 mL/min), R_t = 75 and 90 min, yielding each enantiomer in 100% *ee*.

3,3-Dimethyl-4-methylenebicyclo[3.1.0]hexan-2-one (18): Methyltriphenylphosphonium bromide (26.5 g, 74 mmol) was dissolved in anhydrous diethyl ether (140 mL) under argon, and a commercial solution of *n*-butyllithium in hexane (15%, 1.6 mol, 42.1 mL, l, 67 mmol) was added. The reaction mixture was heated for 1 h under reflux, cooled to room temp., and a solution of 3,3-dimethylbicyclo[3.1.0]hexane-2,4-dione[30] (9.3 g, 67 mmol) in ether (20 mL) was added. After stirring for 12 h at room temp., the reaction mixture was hydrolyzed with a few mL of water. The organic layer was separated, the solvent evaporated, and the residue chromatographed on silica gel (pentane). 3,3-Dimethyl-4-methylenebicyclo[3.1.0]hexan-2-one (**18**) (4.5 g, 49%) was obtained in addition to 3,3-dimethyl-2,4-dimethylenebicyclo[3.1.0]hexane and unchanged 3,3-dimethylbicyclo[3.1.0]hexane-2,4-dione. A small amount was further purified by preparative GC (DC 200, 2 m, 10%, 100 °C, R_t = 7 min). − MS (70 eV); *m*/*z* (%): 136 (20) [M$^+$], 121 (5), 108 (6), 93 (100), 77 (52), 68 (23), 53 (61). − ^{1}H NMR (400 MHz, $CDCl_3$): δ = 1.02 (m, 1 H), 1.18 (s, 3 H), 1.22 (s, 3 H), 1.45 (m, 1 H), 2.25 (m, 1 H), 2.62 (m, 1 H), 5.00 (s, 1 H), 5.20 (s, 1 H).

(*E*)-2-Benzylidene-3,3-dimethyl-4-methylenebicyclo-[3.1.0]hexane [(*E*)-17]: A commercial solution of *n*-butyllithium in hexane (15%,15 mL, 1.6 mol/L, 24 mmol) was diluted with anhydrous THF (75 mL) and the solution was cooled to −70 °C under argon. A solution of benzyl isocyanide[31] (2.8 g, 24 mmol) in THF (15 mL) was added slowly. To the deep red solution was added a solution of 3,3-dimethyl-4-methylenebicyclo[3.1.0]hexan-2-one (**18**) (3.3 g, 24 mmol) in anhydrous THF (25 mL). The reaction mixture was allowed to warm to room temp. and the solvent was removed. Water (50 mL) was added and the mixture was extracted with ether. The combined organic layers were dried with $MgSO_4$. After evaporation of the solvent, silica gel chromatography of the residue (pentane) afforded 0.5 g (10%) of (*E*)-2-benzylidene-3,3-dimethyl-4-methylenebicyclo[3.1.0]hexane [(*E*)-**17**]. − MS (70 eV); *m*/*z* (%): 210 (21) [M$^+$], 195 (35), 180 (34), 165 (73), 152 (23), 141 (20), 129 (27), 119 (100), 115 (50), 105 (57), 91 (82), 89 (67), 78 (52), 65 (35), 51 (47), 39 (71). − ^{1}H NMR (400 MHz, $CDCl_3$): δ = 0.55 (q, 1 H), 1.08 (s, 3 H), 1.20 (s, 3 H), 1.28 (dt, 1 H), 2.20 (m, 1 H), 2.35 (m, 1 H), 4.78 (s, 1 H), 4.98 (s, 1 H), 6.15 (s, 1 H), 7.18 (t, 1 H, phenyl-*para*), 7.33 (t, 2 H, phenyl-*meta*), 7.50 (d, 2 H, phenyl-*ortho*). − ^{13}C NMR (HMQC, 200 MHz, $CDCl_3$): δ = 16.2 (couples with the peak at δ = 1.08/0.55, 2 H of the ^{1}H NMR), 23.3 (1 H,

2.35), 26.2 (1 H, 2.20), 30.8 (3 H, 1.20), 31.0 (3 H, 1.08), 102.3 (2 H, 4.98/4.78), 118.6 (1 H, 6.15), 124.9 (1 H, 7.18), 127.2 (1 H, 7.33), 127.2 (1 H, 7.50). − IR (neat): $\tilde{\nu}$ = 3080 cm^{-1}, 3030, 2980, 2970, 2930, 2870, 1640, 1600, 1495, 1465, 1440, 1360, 1265, 1190, 1170, 1160, 1070, 1030, 925, 875, 800, 745, 700, 685. − The separation of the enantiomers was achieved by HPLC using a Chiralcel OD-H (Baker) column and hexane as the eluent {flow: 0.25 mL/min, column temp. 0 °C, R_t[(−)-(*E*)-**17**] = 62 min, R_t[(+)-(*E*)-**17**] = 71 min}, yielding the enantiomers in *ee*s > 95%.

(*Z*)-2-Benzylidene-3,3-dimethyl-4-methylenebicyclo-[3.1.0]hexane [(*Z*)-17]: (*E*)-2-Benzylidene-3,3-dimethyl-4-methylenebicyclo[3.1.0]hexane [(*E*)-**17**] (0.1 g) was dissolved in 1 mL of hexane and the solution was irradiated (Philips HPK 125 W) for 40 min. The reaction mixture {(*Z*)-**17**/(*E*)-**17** = 4:1, analyzed by analytical GC, OV-1, 50 m, 130 °C, R_t[(*Z*)-**17**] = 28.0 min, R_t[(*E*)-**17**] = 30.8 min} was concentrated and separated by HPLC into the geometric and optical isomers using a Chiralcel OD-H (Baker) column and hexane as the eluent {flow: 0.25 mL/min, column temp.: 0 °C, R_t[(−)-(*E*)-**17**] = 62 min, R_t[(−)-(*Z*)-**17**] = 65 min, R_t[(+)-(*E*)-**17**] = 71 min, R_t[(+)-(*Z*)-**17**] = 161 min}. By collection of the peak with R_t = 161 min, (+)-(*Z*)-**17** was obtained in *ee* > 99%. − MS (70 eV); *m*/*z* (%): 210 (21) [M^+], 195 (35), 180 (34), 165 (73), 152 (23), 141 (20), 129 (27), 119 (100), 115 (50), 105 (57), 91 (82), 89 (67), 78 (52), 65 (35), 51 (47), 39 (71). − ^{1}H NMR (400 MHz, $CDCl_3$): δ = 0.60 (q, 1 H), 0.90 (dt, 1 H), 1.21 (s, 3 H), 1.30 (s, 3 H), 2.10 (dd, 2 H), 4.80 (s, 1 H), 5.08 (s, 1 H), 6.73 (s, 1 H), 7.1−7.3 (m, 5 H).

6-Chloro-6-methylbicyclo[3.1.0]hexan-2-one Ethylene Ketal: Cyclopenten-3-one ethylene ketal[32] (20.0 g, 0.159 mol) and 1,1-dichloroethane (32.7 g, 0.318 mol) were dissolved in anhydrous pentane (40 mL) and the solution was cooled to −40 °C. Under argon, a commercial solution of *n*-butyllithium in hexane (15%, 199 mL, 1.6 mol/L, 0.318 mol *n*BuLi) was added at such a rate that the temp. did not rise above −30 °C. The reaction mixture was warmed to −20 °C, stirred for an additional 30 min, and hydrolyzed with 100 mL of water. The organic layer was separated after addition of 200 mL of ether and 200 mL of water, the aqueous layer was extracted with ether, and the combined organic layers were washed with water and dried with $MgSO_4$. 6-Chloro-6-methylbicyclo[3.1.0]-hexan-2-one ethylene ketal (13.5 g, 45%) was obtained after removal of the solvent. The crude product was used in the next step without further purification. − ^{1}H NMR (80 MHz, C_6D_6): δ = 1.6 (s, 3 H), 1.5−2.2 (m, 6 H), 3.9 (s, 4 H). − MS; *m*/*z* (%): 188 (1) [M^+], 153 (35), 86 (100).

6-Methylenebicyclo[3.1.0]hexan-2-one (22): 6-Chloro-6-methylbicyclo[3.1.0]hexan-2-one ethylene ketal (9.2 g, 0.049 mol) was added dropwise under argon at room temp. over 30 min to a solution of potassium *tert*-butoxide (11.0 g, 0.098 mol) in DMSO (61 mL). The reaction mixture was heated to 90 °C for 90 min and poured after cooling onto 200 g of ice. After addition of 200 mL of ether, the organic layer was separated, the aqueous layer was extracted with ether, and the combined organic layers were washed with water. After removal of the solvent and addition of H_2SO_4 (5%), the reaction mixture was vigorously stirred for 30 min. The organic layer was separated, the aqueous layer was extracted with ether, and the combined organic layers were neutralized with $NaHCO_3$ and dried with $MgSO_4$. After removal of the solvent, 6-methylenebicyclo[3.1.-0]hexan-2-one (**22**) (2.4 g, 45%) was obtained. − MS; *m*/*z* (%): 109 (2) [M^+ + 1], 108 (23) [M^+], 107 (27), 80 (50), 79 (100), 76 (28), 67 (24), 51 (25), 39 (60). − ^{1}H NMR (80 MHz, $CDCl_3$): δ = 1.9−2.3 (m, 5 H), 2.5 (m, 1 H), 5.5 (m, 2 H).

6-Methylenebicyclo[3.1.0]hexan-2-ol: Lithium aluminium hydride (26.4 mg, 0.7 mmol) was suspended in ether (10 mL) under argon and 6-methylenebicyclo[3.1.0]hexan-2-one (**22**) (0.3 g, 2.8 mmol) in ether (10 mL) was added dropwise over 15 min. The mixture was stirred for 30 min at room temp. After hydrolysis (saturated solution of Na_2SO_4), the organic layer was separated and dried with $MgSO_4$. 6-Methylenebicyclo[3.1.0]hexan-2-ol (0.2 g) was obtained after removal of the solvent. − MS; *m*/*z* (%): 110 (14) [M^+], 109 (88), 95 (79), 91 (70), 81 (70), 68 (69), 67 (74), 53 (52), 41 (58), 39 (100). − ^{1}H NMR (80 MHz, $CDCl_3$): δ = 1.4−2.5 (m, 7 H), 4.5 (m, 1 H), 5.5 (m, 2 H).

6-Methylene-2-(2-nitrophenylselanyl)bicyclo[3.1.0]-hexane (23): 6-Methylenebicyclo[3.1.0]hexan-2-ol (0.2 g, 1.82 mmol) and 2-nitrophenyl selenocyanate (0.45 g, 2.0 mmol) were dissolved under argon in anhydrous THF (15 mL). After dropwise addition of tri-*n*-butylphosphane (0.44 g, 2.2 mmol), the mixture was stirred for an additional 90 min. After evaporation of the solvent, the residue was chromatographed on silica gel, using hexane/ether (10:1). − ^{1}H NMR (400 MHz, $CDCl_3$): δ = 1.5−2.2 (m, 6 H), 3.9 (m, 1 H, CHSe), 5.5 (m, 2 H), 7.1−7.7 (m, 3 H), 8.25 (m, 2 H).

6-Methylenebicyclo[3.1.0]hex-2-ene (21): 6-Methylene-2-(2-nitrophenylselanyl)bicyclo[3.1.0]hexane (**23**) (80 mg) was dissolved in $CDCl_3$ (1 mL) and the solution was cooled to −20 °C. After addition of pyridine (44 μL), a solution of hydrogen peroxide (150 μL, 17% H_2O_2, saturated with NaCl) was added. The solution was stirred for 30 min at −20 °C, washed twice at −20 °C with a saturated solution of NaCl, and characterized by a low-temp. ^{1}H NMR spectrum (−40 °C). − ^{1}H NMR (400 MHz, $CDCl_3$): δ = 2.75 (m, 2 H), 5.10 (s, 1 H), 5.15 (s, 1 H),5.40 (m, 1 H), 5.82 (m, 1 H). − The two cyclopropane protons could not be identified because of impurities.

2-*sec*-Butyl[1,3]dithiane: 2-Methylbutyraldehyde (18 g, 0.209 mol) and $ZnCl_2$ (42 g, 0.308 mol) were dissolved in anhydrous ether (100 mL) and the solution was cooled to 0 °C. Over 1 h, 1,3-dimercaptopropane (33.8 g, 0.313 mol) was added dropwise. The solution was allowed to warm to room temp. and stirred for an additional 2 h. After addition of 100 mL of water, the organic layer was separated and the aqueous layer extracted with ether. The combined organic layers were washed with water and dried with $MgSO_4$. After removal of the solvent, 2-*sec*-butyl[1,3]dithiane (30 g, 81%) was obtained, and was used for the next step without further purification. − MS; *m*/*z* (%): 176 (13) [M^+], 147 (2) [M^+ − Et], 121 (10), 119 (100) [M^+ − *s*Bu], 106 (5), 85 (7), 73 (13), 59 (10), 45 (42), 41 (48). − ^{1}H NMR (200 MHz, $CDCl_3$): δ = 0.94 (t, 3 H), 1.09 (d, 3 H), 1.3−2.2 (m, 5 H), 2.9 (m, 4 H), 4.17 (d, 1 H).

2-*sec*-Butyl-2-trimethylsilyl[1,3]dithiane: 2-*sec*-Butyl[1,3]dithiane (28.9 g, 0.164 mol) was dissolved under argon in anhydrous THF (400 mL). After this had been cooled to −25 °C, a commercial solution of *n*-butyllithium (15%, 1.6 mol/L in hexane, 102 mL, 0.163 mol) was added over 45 min and the mixture was stirred for an additional 2 h at −25 °C. A solution of freshly distilled trimethylsilyl chloride (19.6 g, 0.18 mol) in THF (200 mL) was added over 45 min and the solution was stirred for an additional 2 h at −25 °C and 16 h at room temp. After hydrolysis with 50 mL of water and conventional workup, 2-*sec*-butyl-2-trimethylsilyl[1,3]dithiane (35.5 g, 87%) was obtained and used in the next step without further purification. − MS; *m*/*z* (%): 248 (6) [M^+], 233 (5) [M^+ − Me], 191 (20) [M^+ − *s*Bu], 175 (65) [M^+ − Me_3Si], 143 (25), 119 (9), 117 (9), 101 (23), 100 (22), 73 (100) [Me_3Si^+], 45 (50). − ^{1}H NMR (200 MHz, $CDCl_3$): δ = 0.15 (s, 9 H), 0.90 (t, 3 H), 1.14 (d, 3 H), 1.3−2.2 (m, 5 H), 2.9 (m, 4 H). − IR (neat): $\tilde{\nu}$ = 2960 cm^{-1},

2930, 2900, 2870, 2830, 1460, 1425, 1380, 1270, 1250, 1110, 925, 885, 845, 735, 690.

2-Methyl-1-trimethylsilyl-1-butanone: 2-*sec*-Butyl-2-trimethylsilyl-[1,3]dithiane (20.0 g, 0.081 mol), $HgCl_2$ (65.6 g, 0.24 mol), and $CaCO_3$ (40.0 g, 0.40 mol) were heated for 6 h in aqueous acetone (500 mL) with exclusion of light. The solid mercury salts were separated by filtration and washed a few times with chloroform. The combined organic layers were washed with water and dried with $MgSO_4$. After removal of the solvent, the residue was distilled (30 Torr, 60 °C) yielding 2-methyl-1-trimethylsilyl-1-butanone (9.2 g 72%). − MS; *m*/*z* (%): 158 (2) [M^+], 143 (1) [M^+ − Me], 130 (1, McLafferty rearrangement), 115 (1), 101 (3), 73 (100) [TMS^+], 57 (5), 45 (24). − ^{1}H NMR (200 MHz, $CDCl_3$): δ = 0.78 (t, 3 H), 0.90 (d, 3 H), 1.20 (sept, 1 H), 1.65 (sept, 1 H, diastereotop. with respect to H at δ = 1.20), 2.75 (sept, 1 H). − IR (neat): $\tilde{\nu}$ = 2960 cm^{-1}, 2930, 2890, 1740, 1710, 1640, 1460, 1250, 1060, 845, 755, 700.

2-Methyl-1-trimethylsilylbut-1-enyl Triflate:[33] Freshly distilled 2-methyl-1-trimethylsilyl-1-butanone (3.31 g, 0.021 mol) was dissolved under argon in anhydrous dichloromethane (100 mL). After addition of trifluoromethanesulfonic anhydride (6.31 g, 0.022 mol) and 2,6-di-*tert*-butyl-4-methylpyridine (4.73 g, 0.023 mol), the solution was stirred for 10 h. After evaporation of the solvent, the residue was dissolved in pentane, and the solution was separated from solid pyridinium salts and washed with cold 1 M HCl and saturated NaCl solution. After drying with K_2CO_3 and removal of the solvent, the residue was distilled (0.3 Torr, 55 °C), yielding 2-methyl-1-trimethylsilylbutenyl triflate (3.2 g, 58%). The product decomposes quickly at room temp. and was used immediately for the next step. − ^{1}H NMR (200 MHz, $CDCl_3$): δ = 0.14 (s, 9 H), 0.87/0.92 (t/t, 3 H), 1.64/1.68 (s/s, 3 H), 2.00/2.14 (q/q, 2 H, *cis*/*trans* isomers).

1-(1-Methylpropylidene)-1,1a,6,6a-tetrahydrocyclopropa[*a*]-indene (26): Indene (30 g, 0.26 mol) and 2-methyl-1-trimethylsilylbutenyl triflate (2.9 g, 0.011 mol) were dissolved under argon in anhydrous hexane (100 mL). 18-Crown-6 (10 g) and anhydrous potassium fluoride (1.5 g) were added. The milky white solution was stirred for 24 h at room temp. After separation of the solids, the solvent was evaporated and the residue was chromatographed on silica gel, using hexane. The obtained mixture of indene and 1-(1-methylpropylidene)-1,1a,6,6a-tetrahydrocyclopropa[*a*]indene was separated by preparative GC [DC 550, 0.2 m, 110 °C, R_t(indene) = 5 min, R_t{1-(1-methylpropylidene)-1,1a,6,6a-tetrahydrocyclopropa[*a*]indene (**26**) (both isomers)} = 15 min]. − Both isomers: IR (neat): $\tilde{\nu}$ = 3160 cm^{-1} (m), 3120 (s), 2960 (s), 2930(s), 2910 (s), 2870 (s), 2840 (s), 1935 (w), 1900 (w), 1770 (m), 1605 (m), 1580 (w), 1475 (s), 1460 (s), 1440 (m),1430 (m), 1370 (m), 1300 (m), 1250 (m), 1225 (w), 1150 (m), 1040 (m), 1030 (m), 970 (w), 940 (w), 880 (w), 760 (s), 720 (s). − MS; *m*/*z* (%): 184 (6) [M^+], 169 (7) [M^+ − Me], 155 (100) [M^+ − Et], 141 (49), 128 (52), 115 (36), 102 (7), 89 (8), 77 (15), 63 (18), 51 (19), 41 (20), 39 (27). − ^{1}H NMR (200 MHz, C_6D_6): δ = 1.0 (t/t, 3 H), 1.65/1.68 (s/s, 3 H), 2.0 (q/q, 2 H), 2.05/2.10 (t/t, 1 H), 2.70/2.85 (d/d, 1 H), 2.85−3.15 (m, 2 H), 6.9−7.3 (m, 4 H). − ^{13}C NMR (200 MHz, C_6D_6): δ = 11.0, 11.2, 18.4, 18.9, 28.2, 28.4, 17.5, 20.0, 26.1, 27.9, 34.7, 35.5, 121.9, 122.0, 123.1, 123.4, 123.8, 124.1, 124.2, 124.3, 124.4, 125.1, 126.5, 127.0, 141.2, 141.4, 144.4, 144.6. − Separation of the enantiomers was achieved by HPLC, using a Chiralcel OD-H column {Baker, column temp. 5 °C, flow: 0.3 mL/min, UV detector: 254 nm, R_t[(+)-(*Z*)-**26**] = 30.8 min, R_t[(+)-(*E*)-**26**] = 33.4 min, R_t[(−)-(*Z*)-**26**] = 36.9 min, R_t[(−)-(*E*)-**26**] = 38.3 min}, in optical purities of 95% *ee* each. No determination of (*Z*) and (*E*) geometries was possible and the assignment above is arbitrary.

6,6-Dimethyl-1-propenylidene-1,1a,6,6a-tetrahydrocyclopropa[*a*]-indene (37): 1,1-Dimethylindene (**38**) (4.17 g, 28.95 mmol) was dissolved under argon in anhydrous pentane (50 mL). After addition of potassium *tert*-butoxide (6.73 g, 60.0 mmol), 3-bromo-1-butyne (7.70 g, 57.9 mmol) was added dropwise at −15 °C over 60 min. The solution was stirred for an additional 60 min at −15 °C and then allowed to warm to room temp. over 1 h. The mixture was hydrolyzed with saturated NaCl solution (25 mL). The organic layer was separated and the aqueous layer was extracted twice with ether. The combined organic layers were washed with water and dried with $MgSO_4$. After filtration through Florisil, the deep red solution was concentrated at 8 mbar. The residue was separated into the *exo* and *endo* isomers by HPLC, using a Supersphere Si 60 column (22.5 × 2.5 cm) with 15 mL·min^{-1} hexane as eluent and a UV detector at 254 nm. − *exo* isomer: ^{1}H NMR (400 MHz, $CDCl_3$): δ = 1.34 (s, 3 H), 1.41 (s, 3 H), 1.60 (d, 3 H), 2.54 (dd, 1 H), 3.27 (dd, 1 H), 5.27 (m, 1 H), 7.11 (m, 3 H), 7.28 (m, 1 H). − ^{13}C NMR (100 MHz, $CDCl_3$): δ = 15.10, 15.19, 31.15, 35.85, 46.91, 86.69, 88.89, 123.26, 123.47, 126.06, 126.43, 142.78, 151.06, 189.14. − MS (70 eV); *m*/*z* (%): 196 (36) [M^+], 181 (100), 166 (80), 165 (85), 153 (16), 152 (16), 141 (12), 128 (13), 115 (12), 89 (6), 76 (4), 39 (4). − *endo* isomer: ^{1}H NMR (400 MHz, $CDCl_3$): δ = 1.32 (s, 3 H), 1.38 (s, 3 H), 1.73 (d, 3 H), 2.55 (dd, 1 H), 3.29 (dd, 1 H), 5.12 (m, 1 H), 7.07 (m, 1 H), 7.12 (m, 2 H), 7.25 (m, 1 H). − ^{13}C NMR (100 MHz, $CDCl_3$): δ = 15.15, 15.21, 25.30, 30.43, 35.45, 47.26, 86.60, 89.15, 123.32, 123.50, 126.18, 126.53, 142.76, 150.96, 189.18. − MS (70 eV); *m*/*z* (%): 196 (36) [M^+], 181 (100), 166 (80), 165 (85), 153 (16), 152 (16), 141 (12), 128 (13), 115 (12), 89 (6), 76 (4), 39 (4).

1-(7-Bromobicyclo[4.1.0]hept-2-en-7-yl)-1-phenylmethanol (44): A solution of 7,7-dibromobicyclo[4.1.0]hept-2-ene (**42**)[34] (5.0 g, 19.8 mmol) in anhydrous THF (150 mL) was cooled to −120 °C. *n*-Butyllithium in hexane (12.4 mL, 1.6 M, 19.8 mmol) was added over 5 min and, after an additional 5 min, benzaldehyde (2.1 g, 19.8 mmol) was added at the same rate. The reaction mixture was allowed to warm to room temp. overnight and hydrolyzed with water (100 mL) at 0 °C. The organic layer was separated and the aqueous layer extracted four times with pentane (60 mL). The combined organic layers were washed to neutrality and dried with $MgSO_4$. After removal of the solvent, white crystals were formed, and these were recrystallized from pentane/ether (99:1) and dried under vacuum (oil pump). Yield: 3.4 g (12.18 mmol, 62%). − ^{1}H NMR (400 MHz, $CDCl_3$): δ = 1.92 (m, 1 H), 1.98−2.12 (m, 3 H), 2.19 (m, 2 H), 2.34 (d, 1 H, OH), 4.57 + 4.58 (s, 0.5 H each), 7.27 (1 H), 7.35 (2 H), 7.43 (2 H). − ^{13}C NMR (100 MHz, $CDCl_3$): δ = 16.23, 21.57, 25.48, 26.19, 51.4, 71.82, 122.74, 126.05, 127.26, 127.97, 129.63, 142.35. − IR (neat): $\tilde{\nu}$ = 3350 cm^{-1}, 3090, 3065, 3030, 2930, 2900, 2845, 1605, 1490, 1455, 1400, 1385, 1350, 1340, 1275, 1200, 1180, 1130, 1120, 1100, 1080, 1065, 1045, 1030, 850, 760, 725, 705, 695. − MS (70 eV); *m*/*z* (%): 278, 280 (9, 9) [M^+], 234, 236 (4, 4), 210 (100), 208 (92), 199 (46), 181 (56), 164, 166 (33, 33), 129 (95), 107 (59), 91 (51), 79 (91), 77 (72), 65(18), 51 (22), 39 (25), 27 (12).

(7-Bromobicyclo[4.1.0]hept-2-en-7-yl)(phenyl)methyl Trimethylsilyl Ether (45): Bromo alcohol **44** (4.6 g, 16.5 mmol) was dissolved in pyridine (50 mL, freshly distilled from KOH). Hexamethyldisilazane (1.34 g, 8.3 mmol) was added under argon at room temp. over 5 min, after which chlorotrimethylsilane (1.85 g, 17.02 mmol, freshly distilled from molecular sieves) was added at the same rate. The reaction mixture was stirred for an additional 2.5 h and hydrolyzed with water (35 mL) while cooling with ice. After separation, the aqueous layer was extracted four times with pentane (50 mL) and the combined organic layers were washed four times with water.

The organic solution was dried with $MgSO_4$. During the removal of the solvent, one diastereomer of the α-bromo silyl ether crystallized. The white needles were isolated by using a microfrit (G4), washed with a small amount of cold methanol, and recrystallized. Yield: 2.7 g (7.68 mmol, 93%). − ^{1}H NMR (400 MHz, $CDCl_3$): δ = 0.30 (s, 9 H, 3·H_3CSi), 1.85−1.95 (m, 2 H), 1.93−2.16 (m, 3 H), 2.22 (m, 1 H), 4.61 (s, 1 H), 7.38 (dt, 1 H), 6.11 (m, 1 H), 7.21−7.41 (m, 6 H, phenyl). − ^{13}C NMR (100 MHz, $CDCl_3$): δ = 0.99 [prim. 3·Si(CH_3)$_3$], 16.14, 21.72, 25.24, 26.97, 52.10, 73.39, 124.24, 127.20, 127.34, 127.41, 128.58, 143.06. − IR (film): $\tilde{\nu}$ = 3090 cm^{-1}, 3060, 3030, 2950, 2845, 1643, 1603, 1495, 1450, 1400, 1385, 1346, 1250, 1195, 1123, 1093, 1070, 1028, 915, 890, 840, 780, 752, 720, 700, 630, 610. − MS (70 eV); *m/z* (%): 350, 352 (0.4, 0.4) [M$^+$], 284, 286 (0.5, 0.5), 271 (28), 227, 229 (4, 4), 218 (6), 199, 201 (4, 4), 179 (39), 166, 168 (23, 23), 142 (35), 91 (12), 73 (100).

(*Z*)-7-Benzylidenebicyclo[4.1.0]hept-2-ene [(*Z*)-40]: A hexane solution of *tert*-butyllithium (1.1 mL, 1.6 M, 1.76 mmol) was added over 15 min, at −100 °C under argon, to a solution of the α-bromo silyl ether **45** (0.51 g, 1.45 mmol) in anhydrous pentane/THF (1:1, 16 mL). The solution was allowed to warm to room temp. overnight and hydrolyzed with water (15 mL) while cooling with ice. After separation, the aqueous layer was extracted four times with pentane. The combined organic layers were washed three times with water (2 mL), dried with $MgSO_4$, and the solvent was removed. Yield: 0.22 g (1.2 mmol, 83%) of (*Z*)-7-benzylidenebicyclo[4.1.0]hept-2-ene (**40**). − ^{1}H NMR (400 MHz, C_6D_6): δ = 1.25 (m, 1 H), 1.66 (m, 1 H), 1.77−1.88 (m, 3 H), 2.04 (dd, 1 H), 5.52 (m, 1 H), 6.13 (m, 1 H), 6.65 (s, 1 H), 7.09 (t, 1 H), 7.24 (t, 2 H), 7.51 (d, 2 H). − ^{1}H NMR NOE difference spectrum (400 MHz, C_6D_6): irradiated at δ = 6.7 (8-H) => δ = 1.85 (6-H), irradiated at δ = 6.1 (2-H) => δ = 7.4 (10-H). − ^{13}C NMR (100 MHz, C_6D_6): δ = 15.46, 16.09, 17.39, 21.39, 118.87, 125.06, 125.32, 127.12, 127.24, 128.45, 128.70, 137.80. − MS (70 eV); *m/z* (%): 182 (52) [M$^+$], 167 (100), 165 (66), 153 (92), 141 (37), 128 (53), 115 (52), 104 (41), 91 (73), 77 (46), 63 (35), 51 (43), 39 (48), 27 (28). − UV: λ_{max} = 198.9 nm.

(*E*)-7-Benzylidenebicyclo[4.1.0]hept-2-ene [(*E*)-40]: A solution of (*Z*)-**40** in octane (10%) was heated under reflux under argon for 5 h. A 1:1 mixture of the (*Z*) and (*E*) diastereomers was formed and separated by HPLC. − ^{1}H NMR (400 MHz, C_6D_6): δ = 1.31 (m, 1 H), 1.57 (m, 1 H), 1.75 (m, 1 H), 2.2 (m, 2 H), 5.50 (ddd, 1 H), 6.10 (m, 1 H), 6.79 (s, 1 H), 7.10 (t, 1 H), 7.23 (t, 2 H), 7.43 (d, 2 H). − ^{1}H NMR NOE difference spectrum (400 MHz, C_6D_6): irradiated at δ = 6.8 (8-H) => δ = 6.1 (2-H). − ^{13}C NMR (100 MHz, C_6D_6): δ = 13.61, 17.31, 18.76, 21.75, 120.39, 124.28, 126.27, 127.03, 127.09, 128.83, 130.88, 137.92. − MS (70 eV); *m/z* (%): 182 (50) [M$^+$], 167 (100), 165 (57), 153 (56), 141 (15), 128 (32), 115 (24), 104 (19), 91 (42), 77 (22), 63 (11), 51 (15), 39 (22), 27 (13).

Preparative Thermolysis of 7-Benzylidenebicyclo[4.1.0]-hept-2-ene (40): This was carried out using a 45-cm thermolysis tube (i.d. = 2 cm) filled with quartz chips over $^3/_4$ of its length and heated to 350 °C. A pentane solution of the substrate (10%) was added dropwise into a stream of argon (8 mL/s) passing through the tube and the thermolysis products were collected in two consecutive traps cooled at −78 °C.

Preparative HPLC Separation of the Thermolysis Products: Separation of the thermolysis products was achieved by preparative HPLC, using a Supersphere® Si 60-column (4 m, 250 mm × 20 mm) with hexane as eluent (15 mL/min, 36 bar, UV detection: 254 nm). Injected amount: 250-μL portions of a solution in pentane (5%). R_t{(*Z*)-7-benzylidenebicyclo[4.1.0]hept-2-ene [(*Z*)-**40**]} = 19 min, R_t{(*E*)-7-benzylidenebicyclo[4.1.0]hept-2-ene [(*E*)-**40**]} = 21 min, R_t[3-benzylidene-1,4,6-heptatriene (**48**)] = 12 min, R_t[5-phenyl-4-vinyl-1,3-cyclohexadiene (**49**)] = 28 min, R_t{(*E*)-2-benzylidenebicyclo[3.1.0]hept-3-ene (**47**)} = 15 min, R_t{(*Z*)-2-benzylidenebicyclo[3.1.0] hept-3-ene (**46**)} = 17 min. − 5-Phenyl-4-vinyl-1,3-cyclohexadiene (**49**): ^{1}H NMR (400 MHz, C_6D_6): δ = 2.29 (ddd, 1 H), 2.71 (ddd, 1 H), 3.72 (d, 1 H), 4.98 (d, J = 11.0 Hz, 1 H), 5.20 (d, J = 17.0 Hz, 1 H), 5.57 (m, 1 H), 6.02 (m, 1 H), 6.13 (d, 1 H), 6.44 (dd, 1 H), 7.18−7.30 (m, 5 H, phenyl). − ^{13}C NMR (100 MHz, C_6D_6): δ = 32.67, 37.83, 113.29, 125.13, 125.61, 126.33, 126.61, 127.67, 128.58, 137.63, 138.09. − MS (70 eV); *m/z* (%): 182 (27) [M$^+$], 167 (49), 165 (39), 152, (29), 128 (30), 115 (34), 104 (93), 91 (100), 77 (46), 63 (22), 51 (44), 39 (26), 27 (21). − (*E*)-2-Benzylidenebicyclo[3.1.0]hept-3-ene (**47**): ^{1}H NMR (400 MHz, C_6D_6): δ = 1.64 (m, 1 H), 1.95 (m, 1 H), 2.15 (m, 1 H), 2.45 (m, 1 H), 3.25 (m, 1 H), 3.55 (m, 1 H), 6.09 (dd, 1 H), 6.37 (d, 1 H), 6.40 (s, 1 H), 7.12 (t, 1 H), 7.26 (d, 2 H), 7.32 (d, 2 H). − ^{13}C NMR (100 MHz, C_6D_6): δ = 25.15, 26.37, 39.31, 45.81, 114.35, 120.25, 126.25, 127.76, 128.68, 137.64, 140.79, 142.38. − MS (70 eV); *m/z* (%): 182 (27) [M$^+$], 167 (13), 165 (13), 154 (77), 153 (100), 141 (5), 139 (4) 128 (14), 115 (13), 104 (7), 91 (12), 89 (14) 76 (33), 63 (18), 51 (25), 39 (20), 27 (8). − (*Z*)-2-Benzylidenebicyclo[3.1.0]hept-3-ene (**46**): ^{1}H NMR (400 MHz, C_6D_6): δ = 1.74 (m, 1 H), 1.92 (m, 1 H), 2.28 (m, 1 H), 2.41 (m, 1 H), 3.24 (m, 1 H), 3.31 (m, 1 H), 6.22 (m, 1 H), 6.29 (s, 1 H), 7.03 (d, 1 H), 7.09 (t, 1 H), 7.20 (t, 2 H), 7.38 (d, 2 H). − MS (70 eV); *m/z* (%): identical with data of (*E*) isomer.

Preparative Separation of the Enantiomers of 7-Benzylidenebicyclo[4.1.0]hept-2-ene (40): This was achieved by preparative HPLC, using a triacetylcellulose Si 60 column (15−25 m, 250 mm 20 mm) and ethanol/water (96:4) as eluent (4.0 mL/min, 20 bar, UV detection: 254 nm). R_t{(+)-(*Z*)-7-benzylidenebicyclo[4.1.0]hept-2-ene} = 34 min, R_t{(−)-(*Z*)-7-benzylidenebicyclo[4.1.0]hept-2-ene} = 54 min, R_t{(+)-(*E*)-7-benzylidenebicyclo[4.1.0]hept-2-ene} = 42 min, R_t{(−)-(*E*)-7-benzylidenebicyclo[4.1.0]hept-2-ene} = 170 min. The HPLC fractions were diluted with equal volumes of water, extracted with pentane, and concentrated, yielding each enantiomer in 100% *ee*.

Acknowledgments

We are grateful to the Deutsche Forschungsgemeinschaft and the Fonds der Chemischen Industrie for their support.

[1] W. R. Roth, M. Winzer, M. Korell, H. Wildt, *Liebigs Ann.* **1995**, 897−919.
[2] C. A. Grob, *Angew. Chem.* **1969**, *81*, 543−554; *Angew. Chem. Int. Ed. Engl.* **1969**, *8*, 535−546.
[3] R. J. Crawford, K. Takagi, *J. Am. Chem. Soc.* **1972**, *94*, 7406−7416.
[4] H. Iwamura, K. Mislow, *Acc. Chem. Res.* **1988**, *21*, 175−182; W. D. Hounshell, L. Iroff, D. J. Iverson, R. J. Wroczynski, K. Mislow, *Isr. J. Chem.* **1980**, *20*, 65−71; J. Siegel, A. Gutirez, W. B. Schweizer, O. Ermer, K. Mislow, *J. Am. Chem. Soc.* **1986**, *108*, 1569−1575.
[5] G. R. Elling, R. C. Hahn, G. Schwab, *J. Am. Chem. Soc.* **1973**, *95*, 5659−5662.
[6] S. N. Deming, S. L. Morgan, *Anal. Chem.* **1973**, *45*, 278A−283A.
[7] W. R. Roth, T. Bastigkeit, *Liebigs Ann.* **1996**, 2171−2183.
[8] M. Winzer, Dissertation, Universität Bochum, **1994**.
[9] W. R. Roth, F.-G. Klärner, H.-W. Lennartz, *Chem. Ber.* **1980**, *113*, 1818−1829.
[10] W. R. Roth, C. Unger, T. Wasser, *Liebigs Ann.* **1996**, 2155−2169.

[11] W. R. Roth, T. Schaffers, M. Heiber, *Chem. Ber.* **1992**, *125*, 739−749.
[12] N. L. Allinger, Y. H. Yuh, J. H. Lii, *J. Am. Chem. Soc.* **1989**, *111*, 8551; N. L. Allinger, Y. H. Yuh, J. H. Lii, *J. Am. Chem. Soc.* **1989**, *111*, 8566; N. L. Allinger, Y. H. Yuh, J. H. Lii, *J. Am. Chem. Soc.* **1989**, *111*, 8576.
[13] W. R. Roth, V. Staemmler, M. Neumann, C. Schmuck, *Liebigs Ann.* **1995**, 1061−1118.
[14] H. Stetter, H.-J. Sandhagen, *Chem. Ber.* **1967**, *100*, 2837−2841.
[15] W. R. Roth, F. Hunold, M. Neumann, F. Bauer, *Liebigs Ann.* **1996**, 1679−1690.
[16] S. Pekulin, J. A. Berson, *J. Am. Chem. Soc.* **1988**, *110*, 8500−8512.
[17] H. A. Brune, P. Lach, G. Schmidtberg, *Chem. Ber.* **1985**, *118*, 2681−2691.
[18] P. J. Stang, G. M. Mangum, D. P. Fox, P. Haak, *J. Am. Chem. Soc.* **1974**, *96*, 4562−4569.
[19] G. Wegener, Dissertation, Universität Bochum, **1977**.
[20] R. Offerhaus, Dissertation, Universität Bochum, **1993**.
[21] M. Korell, Dissertation, Universität Bochum, **1995**.
[22] H. D. Hartzler, *J. Am. Chem. Soc.* **1961**, *83*, 4990; H. D. Hartzler, *J. Am. Chem. Soc.* **1961**, *83*, 4997.
[23] R. Hässig, H. Siegel, D. Seebach, *Chem. Ber.* **1982**, *115*, 1990−1997.
[24] W. R. Roth, F. Bauer, R. Breuckmann, *Chem. Ber.* **1991**, *124*, 2041−2046; W. R. Roth, D. Wollweber, R. Offerhaus, V. Rekowski, H.-W. Lennartz, R. Sustmann, W. Müller, *Chem. Ber.* **1993**, *126*, 2701−2715; W. R. Roth, M. Winzer, H.-W. Lennartz, R. Boese, *Chem. Ber.* **1993**, *126*, 2717−2725; W. R. Roth, M. Winzer, M. Korell, H. Wildt, *Liebigs Ann.*, **1995**, 897−919.
[25] P. J. Robinson, K. A. Holbrook, *Unimolecular Reactions*, Wiley-Interscience, London, **1972**.
[26] M. J. S. Dewar, E. G. Zoebisch, E. F. Healy, J. J. P. Steward, *J. Am. Chem. Soc.* **1985**, *107*, 3902−3909.
[27] W. Grimme, L. Schumachers, W. R. Roth, R. Breuckmann, *Chem. Ber.* **1981**, *114*, 3197−3208.
[28] E. L. Allred, J. Sonnenberg, S. Winstein, *J. Org. Chem.* **1960**, *25*, 26−29.
[29] W. Freierleben, *Angew. Chem.* **1963**, *75*, 576.
[30] B. M. Jacobson, P. Soteropoulos, S. Bahadori, *J. Org. Chem.* **1988**, *53*, 3247−3255; H. Stetter, H.-J. Sandhage, *Chem. Ber.* **1967**, *100*, 2837−2841.
[31] H. M. Walborsky, G. E. Niznik, *J. Org. Chem.* **1972**, *37*, 187−189.
[32] E. W. Garbisch, Jr., *J. Org. Chem.* **1965**, *30*, 2109−2120.
[33] P. J. Stang, W. Treptow, *Synthesis* **1980**, 283−284.
[34] R. M. Coates, L. A. Last, *J. Am. Chem. Soc.* **1983**, *105*, 7322−7326.
[35] J. A. Nelder, R. Mead, *Comput. J.* **1965**, *7*, 308−313.

Received March 16, 2001
[O01127]